Noname manuscript No.
(will be inserted by the editor)

Superconvergent recovery of Raviart–Thomas mixed finite elements on triangular grids

Randolph E. Bank · Yuwen Li

Received: December 25, 2017 / Accepted: date

Abstract For the second lowest order Raviart–Thomas mixed method, we prove that the canonical interpolant and finite element solution for the vector variable in elliptic problems are superclose in the $H(\mathrm{div})$-norm on mildly structured meshes, where most pairs of adjacent triangles form approximate parallelograms. We then develop a family of postprocessing operators for Raviart–Thomas mixed elements on triangular grids by using the idea of local least squares fittings. Super-approximation property of the postprocessing operators for the lowest and second lowest order Raviart–Thomas elements is proved under mild conditions. Combining the supercloseness and super-approximation results, we prove that the postprocessed solution superconverges to the exact solution in the L^2-norm on mildly structured meshes.

Keywords superconvergence, mildly structured grids, mixed methods, Raviart–Thomas elements, second order elliptic equations

Mathematics Subject Classification (2010) 65N30, 65N50

1 Introduction and preliminaries

Gradient recovery methods for Lagrange elements have been studied extensively by many authors, see, e.g., [30,29,3,4,5,27,28,26] and references therein. Let u be the exact solution of Poisson's equation and u_h be the finite element solution from Lagrange elements. In general ∇u_h rather than u_h is the main quantity of interest. Gradient recovery methods aim to get a new approximation $\boldsymbol{p}_h$ to ∇u by postprocessing u_h or ∇u_h. Comparing to ∇u_h, $\boldsymbol{p}_h$ is often H^1-conforming and $\boldsymbol{p}_h$ superconverges to ∇u in some situation. In addition,

R. E. Bank: Department of Mathematics, University of California, San Diego, La Jolla, California 92093-0112. Email:yul739@ucsd.edu
Y. Li: Department of Mathematics, University of California, San Diego, La Jolla, California 92093-0112. Email:yul739@ucsd.edu

$\boldsymbol{p}_h$ can be used to develop a posteriori error estimators. The recovery-based a posteriori error estimators are popular for their simplicity and asymptotic exactness, see, e.g., [4,29,28].

To derive recovery-type superconvergence, a common ingredient is the so-called supercloseness estimate showing that the canonical interpolant and finite element solution are superclose in some norm. In this paper, we consider the RT_1 mixed method for the second order elliptic equation, namely, (1.5) with $r = 1$. We shall prove that the canonical interpolant $\Pi_h^1\boldsymbol{p}$ and the finite element solution $\boldsymbol{p}_h^1$ are superclose in the $H(\mathrm{div})$-norm under mildly structured grids, i.e., most pairs of adjacent triangles in grids form $O(h^{1+\alpha})$-approximate parallelograms except for a region with measure $O(h^\beta)$, see Definitions 2.1 and 2.2. The supercloseness result in this paper generalizes a result for the RT_0 mixed method in [19]. For Poisson's equation, Brandts [7] proved a supercloseness estimate for RT_1 on three-line grids, i.e., each edge in grids is parallel to one of three fixed lines.

To relax the restriction on mesh structures in supercloseness analysis, we give a constructive proof for Theorem 3.2 instead of using the odd-even argument and the Bramble–Hilbert lemma employed in [6,7]. For Lagrange elements over (α, β)-grids, the authors in [3] transferred the local error $\int_T \nabla(u - u_I)\cdot\nabla v_h$ on each element T to line integrals by the divergence theorem, where u_I is the linear Lagrange interpolant. Then line integrals are grouped in terms of tangential components of ∇v_h by delicate triangular integral identities. However, it's not clear how to handle the local error $\int_T(\boldsymbol{p} - \Pi_h^r\boldsymbol{p})\cdot\boldsymbol{q}_h$ for the RT_r element in a similar fashion. The key observation here is that RT_r elements satisfy the divergence-free property, i.e., $\mathrm{div}(\boldsymbol{p}_{r+1} - \Pi_h^r\boldsymbol{p}_{r+1}) = 0$ on a triangle T, where $\boldsymbol{p}_{r+1} \in \mathcal{P}_{r+1}(T)^2$. Hence $\boldsymbol{p}_{r+1} - \Pi_h^r\boldsymbol{p}_{r+1} = \nabla^\perp w_{r+2}$ for some $w_{r+2} \in \mathcal{P}_{r+2}(T)$ and it can be handled by Green's theorem, see Section 5.

For mixed methods, the finite element solution $\boldsymbol{p}_h$ approximating the vector variable $\boldsymbol{p} \in H(\mathrm{div}, \Omega)$ is the main quantity of physical interest. As far as we know, existing postprocessing/recovery techniques for $\boldsymbol{p}$ and $\boldsymbol{p}_h$ are restricted to strongly structured grids, e.g., three-line, translation invariant and rectangular grids, see, e.g., [11,14,13,7]. As grids become increasingly unstructured, the rate of superconvergence of $\|\boldsymbol{p} - K_h\Pi_h\boldsymbol{p}\|_{0,\Omega}$ deteriorates, where Π_h is the canonical interpolation and K_h is some postprocessing operator. In addition, most of the existing results of recovery methods focus on the lowest order case while the analysis of recovery operators for higher order elements is limited, especially on irregular grids. In this paper, we construct a new family of recovery operators R_h^r for RT_r $(r \geq 0)$ elements by fitting the numerical solution $\boldsymbol{p}_h$ with a vector polynomial of degree $r+1$ in the least squares(LS) sense on each local patch surrounding each vertex in triangular grids. We shall show that R_h^0 and R_h^1 have nice super-approximation property under mild and easy-to-check conditions. The order of approximation of R_h^r is almost independent of the mesh structure. Combining the supercloseness and R_h^r, we finally obtain the superconvergence of the postprocessed solution to the exact solution for RT_0 and RT_1 mixed methods, see Theorem 4.4.

Recovery by local least squares fittings is not a new idea. The famous Zienkiewicz–Zhu(ZZ) superconvergent patch recovery G_h is based on it, see, e.g., [30,29]. For linear elements, $\|\nabla u - G_h\nabla u\| = O(h^2)$ under strongly regular grids (cf. [17]), that is, each pair of adjacent triangles form an $O(h^2)$ approximate parallelogram. Alternatively, Zhang and Naga [28] proposed a different LS-based patch recovery operator G_h^r for Lagrange elements of degree r by postprocessing the scalar function u rather than ∇u. Roughly speaking, $\|\nabla u - G_h^r u\| = O(h^{r+1})$ provided each LS problem has a unique solution on each local patch. R_h^r can be viewed as a Raviart–Thomas version of G_h^{r+1}. In practice, the excellent superconvergence property of G_h^r is attributed to the unique solvability of vertex-based LS problems, which is difficult to prove on unstructured grids. For example, [22] is mainly devoted to the analysis of the uniqueness of the LS solution for G_h^1 on unstructured grids. As far as we know, there is no similar analysis for G_h^r with $r \geq 2$. We shall give a practical criterion of uniqueness for G_h^2 on unstructured grids, which also works for R_h^1, see Theorem 4.1.

For a domain U, the Sobolev seminorms and norms are defined by

$$
\begin{aligned}
&|v|_{k,p,U} = \Big(\int_U |D^k v|^p\Big)^{\frac{1}{p}}, \quad \|v\|_{k,p,U} = \Big(\sum_{m=0}^{k} |v|_{m,p,U}^p\Big)^{\frac{1}{p}},\\
&|v|_{m,U} = |v|_{m,2,U}, \quad \|v\|_{m,U} = \|v\|_{m,2,U},
\end{aligned}
$$

where

$$
|D^k v| := \sum_{\alpha_1+\cdots+\alpha_n=k} \left|\frac{\partial^{\alpha_1+\cdots+\alpha_n}}{\partial x^{\alpha_1}\cdots\partial x^{\alpha_n}} v\right|.
$$

Sobolev norms with ∞-index and norms of vector-valued functions are generalized in usual ways.

In this paper, we consider the second order elliptic equation

$$
\begin{aligned}
-\operatorname{div}(a_2(\boldsymbol{x})\nabla u + \boldsymbol{a}_1(\boldsymbol{x})u) + a_0(\boldsymbol{x})u &= f(\boldsymbol{x}), \quad \boldsymbol{x} \in \Omega, &(1.1a)\\
u &= g(\boldsymbol{x}), \quad \boldsymbol{x} \in \partial\Omega, &(1.1b)
\end{aligned}
$$

where $\operatorname{div} = \nabla\cdot$ is the divergence operator, a_2, a_0 are scalar-valued and $\boldsymbol{a}_1$ is vector-valued. Assume that Ω is simply connected and $a_2, \boldsymbol{a}_1, a_0$ are sufficiently smooth on $\overline{\Omega}$. In addition, $a_2 \geq \Lambda > 0$ for some constant Λ. Let

$$
\begin{aligned}
&\boldsymbol{p} = a_2\nabla u + \boldsymbol{a}_1 u,\\
&a = a_2^{-1}, \quad \boldsymbol{b} = a_2^{-1}\boldsymbol{a}_1, \quad c = a_0.
\end{aligned}
$$

Equation (1.1) is equivalent to the first order system

$$
\begin{aligned}
a\boldsymbol{p} - \boldsymbol{b}u - \nabla u &= 0, \quad \boldsymbol{x} \in \Omega, &(1.2a)\\
-\operatorname{div}\boldsymbol{p} + cu &= f, \quad \boldsymbol{x} \in \Omega, &(1.2b)\\
u &= g, \quad \boldsymbol{x} \in \partial\Omega. &(1.2c)
\end{aligned}
$$

Let $\mathcal{Q} = H(\mathrm{div}, \Omega) := \{\boldsymbol{q} \in L^2(\Omega)^2 : \mathrm{div}\, \boldsymbol{q} \in L^2(\Omega)\}$ and $\mathcal{V} = L^2(\Omega)$. The mixed formulation for (1.2) is to find the pair $\{\boldsymbol{p}, u\} \in \mathcal{Q} \times \mathcal{V}$, such that

$$(a\boldsymbol{p}, \boldsymbol{q}) - (\boldsymbol{q}, \boldsymbol{b}u) + (\mathrm{div}\, \boldsymbol{q}, u) = \langle \boldsymbol{q} \cdot \boldsymbol{n}, g\rangle, \tag{1.3a}$$
$$-(\mathrm{div}\, \boldsymbol{p}, v) + (cu, v) = (f, v), \tag{1.3b}$$

for each pair $\{\boldsymbol{q}, v\} \in \mathcal{Q} \times \mathcal{V}$. Here $\langle \cdot, \cdot\rangle$ denotes the L^2-inner product on $\partial\Omega$.

Let $\mathcal{T}_h$ be a collection of triangles that forms a triangulation of Ω. Let $h_T = |T|^{\frac{1}{2}}$ be the diameter of T and $h = \max_{T\in\mathcal{T}_h} h_T < 1$ be the mesh-size. $\mathcal{T}_h$ is assumed to quasi-uniform, namely, $\max_{T\in\mathcal{T}_h} h_T \le C_0(\min_{T\in\mathcal{T}_h} h_T)$ for some generic constant C_0. The quasi-uniformity implies the minimum angle condition (MAC), namely, there exists a fixed constant $\Theta > 0$, such that $\theta \ge \Theta > 0$ for any angle θ of any triangle $T \in \mathcal{T}_h$. Given a one-dimensional or two-dimensional subset $U \subset \mathbb{R}^2$, let

$$\mathcal{P}_r(U) = \{v : v \text{ is a polynomial on } U \text{ of degree } \le r\}$$

denote the space of polynomials of degree $\le r$. Let $\mathcal{E}_h, \mathcal{E}_h^o, \mathcal{E}_h^\partial$ denote the set of edges, interior edges and boundary edges in $\mathcal{T}_h$, respectively. Let $\mathcal{N}_h$ denote the set of vertices in $\mathcal{T}_h$. Several kinds of local patches are useful for finite element superconvergence analysis. For $\boldsymbol{z} \in \mathcal{N}_h$, let ω_z be the union of triangles in $\mathcal{T}_h$ sharing z as a vertex. For $e \in \mathcal{E}_h$, let ω_e be the union of triangles in $\mathcal{T}_h$ sharing e as an edge. For $T \in \mathcal{T}_h$, let ω_T be the union of T and triangles in $\mathcal{T}_h$ sharing at least one vertex with T. The local nodes, edges , and triangles in U are $\mathcal{N}_h(U) = \{z \in \mathcal{N}_h : z \in \bar{U}\}$, $\mathcal{E}_h(U) = \{e \in \mathcal{E}_h : e \subset \bar{U}\}$, and $\mathcal{T}_h(U) = \{T \in \mathcal{T}_h : T \subset \bar{U}\}$, respectively.

For $r \ge 0$ and $T \in \mathcal{T}_h$, define the space of shape functions

$$\mathcal{RT}_r(T) := \left\{ \begin{pmatrix} v_1 \\ v_2 \end{pmatrix} + v_3 \begin{pmatrix} x_1 \\ x_2 \end{pmatrix} : v_i \in \mathcal{P}_r(T), i = 1, 2, 3 \right\}. \tag{1.4}$$

The RT_r finite element spaces are

$$\mathcal{Q}_h^r := \{\boldsymbol{q}_h \in \mathcal{Q} : \boldsymbol{q}_h|_T \in \mathcal{RT}_r(T),\ \forall T \in \mathcal{T}_h\},$$
$$\mathcal{V}_h^r := \{v_h \in \mathcal{V} : v_h|_T \in \mathcal{P}_r(T),\ \forall T \in \mathcal{T}_h\}.$$

The mixed method for (1.3) is to find $\{\boldsymbol{p}_h^r, u_h^r\} \in \mathcal{Q}_h^r \times \mathcal{V}_h^r$, such that

$$(a\boldsymbol{p}_h^r, \boldsymbol{q}_h) - (\boldsymbol{q}_h, \boldsymbol{b}u_h^r) + (\mathrm{div}\, \boldsymbol{q}_h, u_h^r) = \langle \boldsymbol{q}_h \cdot \boldsymbol{n}, g\rangle, \qquad \boldsymbol{q}_h \in \mathcal{Q}_h^r, \tag{1.5a}$$
$$-(\mathrm{div}\, \boldsymbol{p}_h^r, v_h) + (cu_h, v_h) = (f, v_h), \qquad v_h \in \mathcal{V}_h^r. \tag{1.5b}$$

Under mild assumptions, Douglas and Roberts [12] proved the well-posedness and a priori error estimates for the method (1.5).

Let $|v|_{h,m,U} := \left(\sum_{T\in\mathcal{T}_h} |v|_{m,T}^2\right)^{\frac{1}{2}}$ denote the mesh-dependent semi-norm w.r.t. $\mathcal{T}_h$. $A \lesssim B$ means that $A \le CB$, where C is a generic constant that may change from line to line, and depends only on the shape regularity of $\mathcal{T}_h$ measured by C_0 or Θ. We say $A \approx B$ if $A \lesssim B$ and $B \lesssim A$. The regularity condition will be indicated on right hand sides of estimates. In addition to $\mathcal{Q}_h^r$ and $\mathcal{V}_h^r$, we need the standard nodal finite element space

$$\mathcal{W}_h^r = \{w \in C(\Omega) : w|_T \in \mathcal{P}_r(T),\ \forall T \in \mathcal{T}_h\},$$

where $C(\Omega)$ is the space of continuous functions on Ω. We present two well-known inequalities that will be used in the rest of this paper.

Theorem 1.1 (Interpolation error) *Let $I_h^r : C(\Omega) \to \mathcal{W}_h^r$ denote the Lagrange interpolation of degree r. For $T \in \mathcal{T}_h$ and $r \geq 1$, it holds that*

$$\|v - I_h^r v\|_{0,\gamma,T} \lesssim h^{r+\frac{2}{\gamma}} |v|_{h,r+1,T}, \quad 1 \leq \gamma \leq \infty. \tag{1.6}$$

Theorem 1.2 (Trace inequalities) *For $T \in \mathcal{T}_h$ and $v \in H^1(T)$, it holds that*

$$\|v\|_{0,\partial T} \lesssim h_T^{-\frac{1}{2}} \|v\|_{0,T} + h_T^{\frac{1}{2}} \|\nabla v\|_{0,T}. \tag{1.7}$$

2 Local error expansions

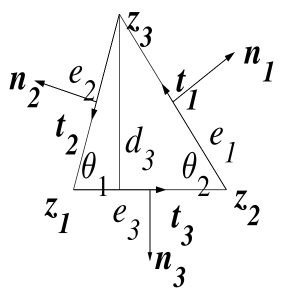

Fig. 1 A local triangle T and associated quantities.

We begin with geometric identities on a local element T. It has three vertices $\{z_k\}_{k=1}^3$, oriented counterclockwise, and corresponding barycentric coordinates $\{\lambda_k\}_{k=1}^3$. Let e_k denote the edge opposite to z_k, θ_k the angle opposite to e_k, ℓ_k the length of e_k, d_k the distance from z_k to e_k, $\boldsymbol{t}_k$ the unit tangent to e_k, oriented counterclockwise, $\boldsymbol{n}_k$ the unit outward normal to e_k, $\partial_{\boldsymbol{t}_k}$ the tangential derivative, $\partial_{\boldsymbol{n}_k}$ the normal derivative, and $\partial^2_{\boldsymbol{t}_k \boldsymbol{n}_k}$ the second mixed derivative, see Figure 1. Corresponding quantities on triangles T' and T'' have superscripts $'$ and $''$ respectively. The subscripts are equivalent mod 3, e.g., $\ell_4 = \ell_1, \theta_0 = \theta_3$.

We have the rotational gradient $\nabla^\perp v = (-\partial_{x_2} v, \partial_{x_1} v)^\intercal$, and the adjoint $\nabla \times \boldsymbol{q} = \partial_{x_1} q_2 - \partial_{x_2} q_1$. $\nabla^\perp$ and $\nabla\times$ are related by Green's formula

$$\int_T \nabla^\perp r \cdot \boldsymbol{q} = \int_{\partial T} r\boldsymbol{q} \cdot \boldsymbol{t} - \int_T r \nabla \times \boldsymbol{q}, \tag{2.1}$$

where $\boldsymbol{t}$ is the unit tangent to ∂K oriented counterclockwise. For $\boldsymbol{v} \in \mathbb{R}^2$, define $\boldsymbol{v}^\perp = (-v_2, v_1)$. Clearly, $\boldsymbol{n}_k^\perp = \boldsymbol{t}_k$, $\boldsymbol{t}_k^\perp = -\boldsymbol{n}_k$.

Now we introduce basic definitions for RT_r elements. For $e \in \mathcal{E}_h$, let $\{(w_j, \boldsymbol{g}_j)\}_{j=1}^{r+1}$ denote the Gaussian quadrature on e, where $\{\boldsymbol{g}_j\}$ are quadrature points and $\{w_j\}$ are corresponding weights. $\{(w_j, \boldsymbol{g}_j)\}_{j=1}^{r+1}$ is exact for $\mathcal{P}_{2r+1}(e)$, i.e.,

$$\int_e v = \sum_{j=1}^{r+1} w_j v(\boldsymbol{g}_j) \text{ for all } v \in \mathcal{P}_{2r+1}(e). \tag{2.2}$$

Let $v_j \in \mathcal{P}_r(e)$ be the polynomial that is w_j^{-1} at $\boldsymbol{g}_j$ and 0 at the rest of quadrature points. For $T \in \mathcal{T}_h$, let $\{\lambda_l\}_{l=1}^{r(r+1)/2}$ be the nodal basis function of Lagrange elements of degree $r-1$ on T ($\{\lambda_l\} = \emptyset$ if $r=0$; $\{\lambda_l\} = \{1\}$ if $r=1$). We can specify degrees of freedom of RT_r elements as

$$\mathcal{N}_e^j(\boldsymbol{q}) := \frac{1}{|e|}\int_e \boldsymbol{q}\cdot\boldsymbol{n}_e v_j, \quad \mathcal{N}_T^{lm}(\boldsymbol{q}) := \frac{1}{|T|}\int_T q_m\lambda_l,$$

where $\boldsymbol{n}_e$ is a unit normal to e, $\boldsymbol{q} = (q_1, q_2)^\intercal$, and $1 \le j \le r+1$, $1 \le l \le r(r+1)/2, m = 1, 2$. By (2.2) and the definition of v_j, we have $\mathcal{N}_e^j(\boldsymbol{q}) = \boldsymbol{q}(\boldsymbol{g}_j)\cdot\boldsymbol{n}_e$ provided $\boldsymbol{q} \in \mathcal{P}_{r+1}(e)^2$. For $\boldsymbol{q} \in H^1(\Omega)^2$, the RT_r interpolant $\Pi_h^r\boldsymbol{q} \in \mathcal{Q}_h^r$ satisfies

$$\mathcal{N}_e^j(\Pi_h^r\boldsymbol{q}) = \mathcal{N}_e^j(\boldsymbol{q}), \quad \mathcal{N}_T^{lm}(\Pi_h^r\boldsymbol{q}) = \mathcal{N}_T^{lm}(\boldsymbol{q}),$$

for all indices j, l, m, and $e \in \mathcal{E}_h, T \in \mathcal{T}_h$. The existence and uniqueness of $\Pi_h^r\boldsymbol{q}$ is always guaranteed. In addition, Π_h^r is stable in the L^∞-norm

$$\|\Pi_h^k\boldsymbol{q}\|_{0,\infty,T} \lesssim \|\boldsymbol{q}\|_{0,\infty,T}, \quad T \in \mathcal{T}_h. \tag{2.3}$$

For $v \in \mathcal{V}$, the interpolant $P_h^r v$ is the L^2-projection of v onto $\mathcal{V}_h^r$. There is a nice commuting property about P_h^r, Π_h^r and div, i.e.,

$$\operatorname{div}(\Pi_h^r\boldsymbol{q}) = P_h^r(\operatorname{div}\boldsymbol{q}), \quad \forall \boldsymbol{q} \in H^1(\Omega)^2. \tag{2.4}$$

The following interpolation error estimates hold, see, e.g., [12].

$$\|\boldsymbol{q} - \Pi_h^r\boldsymbol{q}\|_{0,\Omega} \lesssim h^{r+1}|\boldsymbol{q}|_{h,r+1,\Omega}, \tag{2.5a}$$
$$\|\operatorname{div}(\boldsymbol{q} - \Pi_h^r\boldsymbol{q})\|_{0,\Omega} \lesssim h^{r+1}|\operatorname{div}\boldsymbol{q}|_{h,r+1,\Omega}, \tag{2.5b}$$
$$\|v - P_h^r v\|_{0,\Omega} \lesssim h^{r+1}|v|_{h,r+1,\Omega}. \tag{2.5c}$$

In the rest of this section, we will present variational error expansions for the RT_1 element. Comparing to RT_0, the theory of RT_1 is much more complicated. Let d be the diameter of the circumscribed circle of T. For each edge e_k, there are several associated geometric quantities

$$\begin{aligned}
&\mu_{11,k}^1 = \frac{1}{5760}\big(3\ell_k^4 - 3(\ell_{k-1}^2 - \ell_{k+1}^2)^2 - 4\ell_k^2(\ell_{k-1}^2 + \ell_{k+1}^2)\big),\\
&\mu_{12,k}^1 = \mu_{21,k}^1 = \frac{1}{1440d}\ell_1\ell_2\ell_3(\ell_{k-1}^2 - \ell_{k+1}^2), \quad \mu_{22,k}^1 = -\frac{1}{1440d^2}\ell_1^2\ell_2^2\ell_3^2,\\
&\mu_{11,k}^2 = \frac{1}{2880\ell_1\ell_2\ell_3}d(\ell_{k-1}^2 - \ell_{k+1}^2)\big(4\ell_k^2 - (\ell_{k-1}^2 - \ell_{k+1}^2)^2 - 3\ell_k^2(\ell_{k-1}^2 + \ell_{k+1}^2)\big),\\
&\mu_{12,k}^2 = \mu_{21,k}^2 = -\mu_{11,k}^1, \quad \mu_{22,k}^2 = -\mu_{12,k}^1,
\end{aligned}$$

and second order differential operators $\{\mathcal{D}_{i,k}^{jl}\}_{1\le i,j,l\le 2}$

$$\begin{aligned}
&\mathcal{D}_{1,k}^{11} = \boldsymbol{t}_k \cdot \partial_{\boldsymbol{t}_k}^2, \quad \mathcal{D}_{1,k}^{12} = \mathcal{D}_{1,k}^{21} = \boldsymbol{t}_k \cdot \partial_{\boldsymbol{t}_k \boldsymbol{n}_k}^2, \quad \mathcal{D}_{1,k}^{22} = \boldsymbol{t}_k \cdot \partial_{\boldsymbol{n}_k}^2,\\
&\mathcal{D}_{2,k}^{11} = \boldsymbol{n}_k \cdot \partial_{\boldsymbol{t}_k}^2, \quad \mathcal{D}_{2,k}^{12} = \mathcal{D}_{2,k}^{21} = \boldsymbol{n}_k \cdot \partial_{\boldsymbol{t}_k \boldsymbol{n}_k}^2, \quad \mathcal{D}_{2,k}^{22} = \boldsymbol{n}_k \cdot \partial_{\boldsymbol{n}_k}^2.
\end{aligned}$$

We define the second order differential operator $\mathcal{B}_k(\boldsymbol{q}) := \sum_{i,j,l=1}^2 \mu_{jl,k}^i \mathcal{D}_{i,k}^{jl}(\boldsymbol{q})$. The next lemma is our main tool for estimating the global variational error whose proof is left in Section 5.

Lemma 2.1 *For $\boldsymbol{p}_2 \in \mathcal{P}_2(T)^2$ and $w_2 \in \mathcal{P}_2(T)$,*

$$\int_T (\boldsymbol{p}_2 - \Pi_h^1 \boldsymbol{p}_2) \cdot \nabla^\perp w_2 = \sum_{k=1}^3 \int_{e_k} \mathcal{B}_k(\boldsymbol{p}_2) \partial_{\boldsymbol{t}_k}^2 w_2.$$

Built upon Lemma 2.1, we derive the local error expansion for general $\boldsymbol{p}$.

Theorem 2.1 *For $w_2 \in \mathcal{P}_2(T)$,*

$$\int_T (\boldsymbol{p} - \Pi_h^1 \boldsymbol{p}) \cdot \nabla^\perp w_2 = \sum_{k=1}^3 \int_{e_k} \mathcal{B}_k(\boldsymbol{p}) \partial_{\boldsymbol{t}_k}^2 w_2 + O(h_T^3)|\boldsymbol{p}|_{3,T} \|\nabla^\perp w_2\|_{0,T}.$$

Proof Let $\boldsymbol{p}_I$ be the quadratic interpolant of $\boldsymbol{p}$. By Lemma 2.1, we have

$$\begin{aligned}
\int_T (\boldsymbol{p} - \Pi_h^1 \boldsymbol{p}) \cdot \nabla^\perp w_2 &= \int_T (\mathrm{id} - \Pi_h^1)(\boldsymbol{p} - \boldsymbol{p}_I) \cdot \nabla^\perp w_2\\
&\quad + \sum_{k=1}^3 \int_{e_k} \mathcal{B}_k(\boldsymbol{p}_I - \boldsymbol{p}) \partial_{\boldsymbol{t}_k}^2 w_2 + \sum_{k=1}^3 \int_{e_k} \mathcal{B}_k(\boldsymbol{p}) \partial_{\boldsymbol{t}_k}^2 w_2 \\
&:= I + II + III,
\end{aligned} \tag{2.6}$$

where id is the identity operator. The inequalities (1.6) and (2.3) give the upper bound

$$\begin{aligned}
|I| &\lesssim \|(\mathrm{id} - \Pi_h^1)(\boldsymbol{p} - \boldsymbol{p}_I)\|_{0,T} \|\nabla^\perp w_2\|_{0,T}\\
&\lesssim h_T \|(\mathrm{id} - \Pi_h^1)(\boldsymbol{p} - \boldsymbol{p}_I)\|_{0,\infty,T} \|\nabla^\perp w_2\|_{0,T}\\
&\lesssim h_T \|\boldsymbol{p} - \boldsymbol{p}_I\|_{0,\infty,T} \|\nabla^\perp w_2\|_{0,T}\\
&\lesssim h_T^3 |\boldsymbol{p}|_{3,T} \|\nabla^\perp w_2\|_{0,T}.
\end{aligned} \tag{2.7}$$

Using the trace inequality (1.7), inverse inequality, and $\mu^i_{jl,k} = O(h_T^4)$,

$$
\begin{aligned}
|II| &\lesssim \sum_{k=1}^{3} \|\mathcal{B}_k(\boldsymbol{p}_I - \boldsymbol{p})\|_{0,e_k} \|\partial^2_{\boldsymbol{t}_k} w_2\|_{0,e_k} \\
&\lesssim \sum_{k=1}^{3} \left(h_T^{-\frac{1}{2}} \|\mathcal{B}_k(\boldsymbol{p}_I - \boldsymbol{p})\|_{0,T} + h_T^{\frac{1}{2}} |\mathcal{B}_k(\boldsymbol{p}_I - \boldsymbol{p})|_{1,T}\right) \\
&\qquad \times \left(h_T^{-\frac{1}{2}} \|D^2 w_2\|_{0,T} + h_T^{\frac{1}{2}} |D^2 w_2|_{1,T}\right) \\
&\lesssim \sum_{k=1}^{3} (h_T^{-\frac{1}{2}} |h_T^4(\boldsymbol{p}_I - \boldsymbol{p})|_{2,T} + h_T^{\frac{1}{2}} |h_T^4(\boldsymbol{p}_I - \boldsymbol{p})|_{3,T}) \times (h^{-\frac{3}{2}} \|\nabla^\perp w_2\|_{0,T}) \\
&\lesssim h_T^3 |\boldsymbol{p}|_{3,T} \|\nabla^\perp w_2\|_{0,T}.
\end{aligned}
\tag{2.8}
$$

Combining (2.6)–(2.8) , we prove the theorem. □

Supercloseness estimates in this paper hold on mildly structured grids, see, e.g., [16,3,27,22,15].

Definition 2.1 For $e \in \mathcal{E}_h^o$, let $T, T' \in \mathcal{T}_h$ be the two adjacent elements sharing e. Define $e_1 = e_1' = e$. By going along ∂T and $\partial T'$ counterclockwise, we obtain other two pairs of corresponding edges e_2, e_2' and e_3, e_3'. We say $\omega_e = T \cup T'$ is an $O(h^{1+\alpha})$-approximate parallelogram provided $|e_i| = |e_i'| + O(h^{1+\alpha})$ for $i = 1, 2, 3$.

Definition 2.2 Assume $\mathcal{E}_h^o$ is the disjoint union of two subsets $\mathcal{E}_{h,1}^o$ and $\mathcal{E}_{h,2}^o$. We say the triangulation $\mathcal{T}_h$ satisfies the (α, β)-condition if for each $e \in \mathcal{E}_{h,1}^o$, ω_e an $O(h^{1+\alpha})$-approximate parallelogram, while $\sum_{e \in \mathcal{E}_{h,2}^o} |\omega_e| = O(h^\beta)$.

Although the expression of $\mathcal{B}_k$ is complicated, it suffices to keep the following in mind.

1. $\{\mathcal{B}_k\}_{k=1}^3$ are second order differential operators of magnitude h_T^4:

$$\mathcal{B}_k(\boldsymbol{q}) = O(h_T^4) \sum_{i,j,l=1}^{2} \partial_{x_i} \partial_{x_j} q_l.$$

2. For $e \in \mathcal{E}_h^o$, we have $\omega_e = T \cup T'$. Let $\boldsymbol{t}_e$ denote the unit tangent and and $\boldsymbol{n}_e$ the unit normal to e whose directions are induced by T. Let $\bar{\boldsymbol{a}} = \frac{1}{|T|} \int_T \boldsymbol{a}$ and $\bar{\boldsymbol{a}}' = \frac{1}{|T|} \int_{T'} \boldsymbol{a}$. Let $\mathcal{B}_e$ be the operator based on T and $\mathcal{B}_e'$ based on T'. If ω_e is an $O(h^{1+\alpha})$-approximate parallelogram, then on the edge e, we have the cancellation

$$\bar{\boldsymbol{a}} \mathcal{B}_e(\boldsymbol{q}) - \bar{\boldsymbol{a}}' \mathcal{B}_e'(\boldsymbol{q}) = O(h_e^{4+\min(1,\alpha)}) \sum_{i,j,m=1}^{2} \partial_{x_i} \partial_{x_j} q_m. \tag{2.9}$$

Indeed, ω_e is an approximate parallelogram implies that $\ell_k = \ell'_k + O(h^{1+\alpha})$, $\boldsymbol{t}_k = \boldsymbol{t}'_k + O(h^\alpha)$, $\sin\theta_k = \sin\theta'_k + O(h^\alpha)$, $d = d' + O(h^{1+\alpha})$. Combining these estimates with $\bar{\boldsymbol{a}} = \bar{\boldsymbol{a}}' + O(h)$, (2.9) follows from the telescoping type inequality

$$\left|\prod_{i=1}^n a_i - \prod_{i=1}^n b_i\right| \le \sum_{i=1}^n |a_i - b_i| \prod_{j\ne i} \max(a_j, b_j).$$

3 Supercloseness estimates

In this section, first we prove a superconvergence estimate for variational error which is a foundation of supercloseness estimates.

Lemma 3.1 *Let $\mathcal{T}_h$ satisfy the (α,β)-condition and $\bar{a}$ be the piecewise constant with $\bar{a}|_T = \frac{1}{|T|}\int_T a$ for each $T \in \mathcal{T}_h$. For $w_h \in \mathcal{W}_h^2$, it holds that*

$$(\bar{a}(\boldsymbol{p} - \Pi_h^1 \boldsymbol{p}), \nabla^\perp w_h) \lesssim h^{2+\min(\frac12,\alpha,\frac{\beta}{2})}\big(|\boldsymbol{p}|_{2,\infty,\Omega} + |\boldsymbol{p}|_{3,\Omega}\big)\|\nabla^\perp w_h\|_{0,\Omega}.$$

Proof By Theorem 2.1 and the Cauchy–Schwarz inequality, the left hand side is

$$\begin{aligned}
&(\bar{\boldsymbol{a}}(\boldsymbol{p} - \Pi_h^1 \boldsymbol{p}), \nabla^\perp w_h)\\
&= \sum_{T\in\mathcal{T}_h}\sum_{k=1}^3 \int_{e_k} \bar{a}\mathcal{B}_k(\boldsymbol{p})\partial^2_{\boldsymbol{t}_k} w_h + \sum_{T\in\mathcal{T}_h} O(h_T^3)|\boldsymbol{p}|_{3,T}\|\nabla^\perp w_h\|_{0,T}\\
&= \Big(\sum_{e\in\mathcal{E}^o_{h,1}} + \sum_{e\in\mathcal{E}^o_{h,2}\cup\mathcal{E}^\partial_h}\Big)\int_e \big(\bar{a}\mathcal{B}_e(\boldsymbol{p}) - \bar{a}'\mathcal{B}'_e(\boldsymbol{p})\big)\partial^2_{\boldsymbol{t}_e} w_h\\
&\quad + O(h^3)|\boldsymbol{p}|_{3,\Omega}\|\nabla^\perp w_2\|_{0,\Omega} := I + II + O(h^3)|\boldsymbol{p}|_{3,\Omega}\|\nabla^\perp w_2\|_{0,\Omega}.
\end{aligned} \tag{3.1}$$

Here the notations in (2.9) are adopted and $\mathcal{B}'_e(\boldsymbol{p}) = 0$ if $e \in \mathcal{E}_h^\partial$. By the cancellation (2.9), the trace inequality (1.7), and the inverse inequality,

$$\begin{aligned}
|I| &\lesssim \sum_{e\in\mathcal{E}^o_{h,1}} h^{4+\min(1,\alpha)}\|D^2\boldsymbol{p}\|_{0,e}\|D^2 w_h\|_{0,e}\\
&\lesssim \sum_{e\in\mathcal{E}^o_{h,1}} h^{4+\min(1,\alpha)}\big(h^{-\frac12}\|D^2\boldsymbol{p}\|_{0,T} + h^{\frac12}\|D^3\boldsymbol{p}\|_{0,T}\big)\big(h^{-\frac12}\|D^2 w_h\|_{0,T}\big)\\
&\lesssim \sum_{e\in\mathcal{E}^o_{h,1}} h^{2+\min(1,\alpha)}\|\boldsymbol{p}\|_{3,T}\|\nabla^\perp w_h\|_{0,T}\\
&\lesssim h^{2+\min(1,\alpha)}\|\boldsymbol{p}\|_{3,\Omega}\|\nabla^\perp w_h\|_{0,\Omega}.
\end{aligned} \tag{3.2}$$

For $e \in \mathcal{E}_{h,2}^o$, there is no cancellation. Let $\widetilde{\Omega} = \cup_{e\in\mathcal{E}_{h,2}^o\cup\mathcal{E}_h^\partial}\omega_e$. Using $|\widetilde{\Omega}| = O(h^{\min(1,\beta)})$ and the inverse inequality, the sum over $\mathcal{E}_{h,2}^o$ is

$$\begin{aligned}|II| &\lesssim \sum_{e\in\mathcal{E}_{h,2}^o\cup\mathcal{E}_h^\partial} h^4|D^2\boldsymbol{p}|_{0,\infty,e}\int_e|\partial_{\boldsymbol{t}_k}^2 w_h| \\ &\lesssim h^2|\boldsymbol{p}|_{2,\infty,\Omega}\sum_{e\in\mathcal{E}_{h,2}^o\cup\mathcal{E}_h^\partial}\int_{\omega_e}|\nabla^\perp w_h| \\ &\lesssim h^{2+\min(\frac{1}{2},\frac{\beta}{2})}|\boldsymbol{p}|_{2,\infty,\Omega}\|\nabla^\perp w_h\|_{0,\widetilde{\Omega}}.\end{aligned}\tag{3.3}$$

Combining (3.1)–(3.3) we prove the theorem. □

Subtracting (1.5) from (1.3) gives the error equation

$$(\boldsymbol{a}(\boldsymbol{p}-\boldsymbol{p}_h^r),\boldsymbol{q}_h) - (\boldsymbol{q}_h,\boldsymbol{b}(u-u_h^r)) + (\operatorname{div}\boldsymbol{q}_h, u-u_h^r) = 0, \quad \boldsymbol{q}_h\in\mathcal{Q}_h^r, \tag{3.4a}$$

$$-(\operatorname{div}(\boldsymbol{p}-\boldsymbol{p}_h^r),v_h) + (c(u-u_h^r),v_h) = 0, \quad v_h\in\mathcal{V}_h^r. \tag{3.4b}$$

Douglas and Roberts [12] have shown the standard a priori error estimates:

$$\begin{aligned}&\|\boldsymbol{p}-\boldsymbol{p}_h^r\|_{0,\Omega}\lesssim h^{r+1}\|u\|_{r+2,\Omega},\\ &\|\operatorname{div}(\boldsymbol{p}-\boldsymbol{p}_h^r)\|_{0,\Omega}\lesssim h^{r+1}\|u\|_{r+3,\Omega},\\ &\|u-u_h^r\|_{0,\Omega}\lesssim h^{r+1}\|u\|_{r+1+\delta_{r0},\Omega},\end{aligned}\tag{3.5}$$

where $\delta_{r0}=1$ if $r=0$ and $\delta_{r0}=0$ if $r\neq 0$. In addition, [12] gives the well-known supercloseness result for the scalar unknown u

$$\|P_h^r u - u_h^r\|_{0,\Omega}\lesssim h^{r+2}\|u\|_{r+2+\delta_{r0},\Omega}. \tag{3.6}$$

(3.6) holds on unstructured meshes and implies that $\|\operatorname{div}(\Pi_h^r\boldsymbol{p}-\boldsymbol{p}_h^r)\|_{0,\Omega}$ is supersmall. For convenience, let $\boldsymbol{\xi}_h := \Pi_h^r\boldsymbol{p}-\boldsymbol{p}_h^r$.

Theorem 3.1 *For general shape regular $\mathcal{T}_h$ and $r\geq 0$,*

$$\|\operatorname{div}(\Pi_h^r\boldsymbol{p}-\boldsymbol{p}_h^r)\|_{0,\Omega}\lesssim h^{r+2}\|u\|_{2+r+\delta_{r0},\Omega}.$$

Proof Let

$$v_h := \frac{\operatorname{div}\boldsymbol{\xi}_h}{\|\operatorname{div}\boldsymbol{\xi}_h\|_{0,\Omega}}\in\mathcal{V}_h^r.$$

By (2.4) and (3.4), we have

$$\begin{aligned}\|\operatorname{div}\boldsymbol{\xi}_h\|_{0,\Omega} &= (\operatorname{div}\boldsymbol{\xi}_h, v_h) = (P_h^r\operatorname{div}\boldsymbol{p}-\operatorname{div}\boldsymbol{p}_h^r, v_h)\\ &= (\operatorname{div}(\boldsymbol{p}-\boldsymbol{p}_h^r),v_h) = (u-P_h^r u, cv_h) + (P_h^r u - u_h^r, cv_h).\end{aligned}$$

It then follows from (2.5), (3.5), (3.6), and $\|v_h\|_{0,\Omega}=1$ that

$$\begin{aligned}\|\operatorname{div}\boldsymbol{\xi}_h\|_{0,\Omega} &= (u-P_h^r u, cv_h - P_h^r(cv_h)) + O(h^{r+2})\|u\|_{2+r+\delta_{r0},\Omega}\\ &= O(h^{2r+2})\|u\|_{r+1,\Omega}|cv_h|_{h,r+1,\Omega} + O(h^{r+2})\|u\|_{2+r+\delta_{r0},\Omega}\\ &= O(h^{r+2})\|u\|_{2+r+\delta_{r0},\Omega}.\end{aligned}$$

In the last step, we use $v_h|_T\in\mathcal{P}_r(T)$ and the inverse inequality. □

Before proving the superconvergence estimate of $\|\Pi_h^r \boldsymbol{p} - \boldsymbol{p}_h^r\|_{0,\Omega}$, it is necessary to discuss the L^2 de Rham complex in $\mathbb{R}^2$:

$$H^1(\Omega) \xrightarrow{\nabla^\perp} \mathcal{Q} \xrightarrow{\text{div}} \mathcal{V} \to 0.$$

Here $\mathcal{V} = L^2(\Omega)$ is equipped with the standard $(\cdot,\cdot)$ inner product. Since we are dealing with variable coefficients, $\mathcal{Q}$ is equipped with the weighted L^2 inner product $(\cdot,\cdot)_a$:

$$(\boldsymbol{q}_1, \boldsymbol{q}_2)_a := (a\boldsymbol{q}_1, \boldsymbol{q}_2), \quad \boldsymbol{q}_1, \boldsymbol{q}_2 \in L^2(\Omega)^2.$$

The weighted L^2-norm is $\|\boldsymbol{q}\|_a = (a\boldsymbol{q}, \boldsymbol{q})^{\frac{1}{2}}$. Clearly, $\|\boldsymbol{q}\|_{0,\Omega} \approx \|\boldsymbol{q}\|_a$ for all $\boldsymbol{q} \in L^2(\Omega)^2$. Similarly, we have the discrete subcomplex

$$\mathcal{W}_h^{r+1} \xrightarrow{\nabla^\perp} \mathcal{Q}_h^r \xrightarrow{\text{div}} \mathcal{V}_h^r \to 0. \tag{3.7}$$

Since Ω is simply connected, (3.7) is exact and the discrete Helmholtz/Hodge decomposition (cf. [1,2,9,18]) holds:

$$\mathcal{Q}_h^r = \nabla^\perp \mathcal{W}_h^{r+1} \oplus \text{grad}_h \mathcal{V}_h^r, \tag{3.8}$$

where $\oplus$ denotes the direct sum w.r.t. $(\cdot,\cdot)_a$., $\text{grad}_h : \mathcal{V}_h^r \to \mathcal{Q}_h^r$ is the adjoint of $-\text{div} : \mathcal{Q}_h^r \to \mathcal{V}_h^r$ w.r.t. the weighted inner product $(\cdot,\cdot)_a$, namely, $(a\,\text{grad}_h v_h, \boldsymbol{q}_h) = -(v_h, \text{div}\,\boldsymbol{q}_h)$ for all $\boldsymbol{q}_h \in \mathcal{Q}_h^r$.

The last ingredient for our supercloseness analysis is a discrete Poincaré inequality.

Lemma 3.2

$$\|v_h\|_{0,\Omega} \lesssim \|\text{grad}_h v_h\|_a, \quad v \in \mathcal{V}_h^r.$$

Proof div : $\mathcal{Q}_h^r \to \mathcal{V}_h^r$ is surjective and there exists $\boldsymbol{q}_h \in \mathcal{Q}_h^r$ and $\text{div}\,\boldsymbol{q}_h = v_h$. In addition, Raviart and Thomas [23] have shown that $\|\boldsymbol{q}_h\|_a \approx \|\boldsymbol{q}_h\|_{0,\Omega} \lesssim \|v_h\|_{0,\Omega}$. It then follows

$$\|v_h\|_{0,\Omega}^2 = -(a\,\text{grad}_h v_h, \boldsymbol{q}_h) \lesssim \|\text{grad}_h v_h\|_a \|v_h\|_{0,\Omega},$$

which completes the proof. □

With the above preparations, we are able to prove supercloseness estimates for the RT_1 mixed methods.

Theorem 3.2 *Assume that $\mathcal{T}_h$ satisfies the (α,β)-condition. Then*

$$\|\Pi_h^1 \boldsymbol{p} - \boldsymbol{p}_h^1\| \lesssim h^{2+\min(\frac{1}{2},\alpha,\frac{\beta}{2})} \big(|\boldsymbol{p}|_{2,\infty,\Omega} + \|\boldsymbol{p}\|_{3,\Omega}\big).$$

Proof For simplicity, the super-index $r = 1$ is suppressed in the proof. Consider the discrete Helmholtz decomposition

$$\boldsymbol{\xi}_h := \Pi_h \boldsymbol{p} - \boldsymbol{p}_h = \nabla^\perp w_h \oplus \operatorname{grad}_h v_h, \tag{3.9}$$

for some $\{v_h, w_h\} \in \mathcal{V}_h^1 \times \mathcal{W}_h^2$. Let $\boldsymbol{q}_h = \operatorname{grad}_h v_h / \|\operatorname{grad}_h v_h\|_a$. By Lemma 3.2 and Lemma 3.1,

$$\begin{aligned} \|\operatorname{grad}_h v_h\|_a &= (\operatorname{grad}_h v_h, \boldsymbol{q}_h)_a = -(v_h, \operatorname{div} \boldsymbol{q}_h) \\ &= -\big(v_h, \frac{\operatorname{div} \boldsymbol{\xi}_h}{\|\operatorname{grad}_h v_h\|_a}\big) \lesssim \|\operatorname{div} \boldsymbol{\xi}_h\|_{0,\Omega} \lesssim h^{r+2} \|u\|_{r+2+\delta_{r0}}. \end{aligned} \tag{3.10}$$

It remains to bound $\nabla^\perp w_h$. Let $\boldsymbol{q}_h = \nabla^\perp w_h / \|\nabla^\perp w_h\|_a$. The orthogonality implies

$$\|\nabla^\perp w_h\|_a = -(a(\boldsymbol{p} - \Pi_h \boldsymbol{p}), \boldsymbol{q}_h) + (a(\boldsymbol{p} - \boldsymbol{p}_h), \boldsymbol{q}_h) := I + II. \tag{3.11}$$

I is split as

$$I = ((\bar{a} - a)(\boldsymbol{p} - \Pi_h \boldsymbol{p}), \boldsymbol{q}_h) - (\bar{a}(\boldsymbol{p} - \Pi_h \boldsymbol{p}), \boldsymbol{q}_h).$$

By $\|\bar{a} - a\|_{0,\infty,\Omega} = O(h)$, (2.5) and Lemma 3.1,

$$|I| \lesssim h^3 |\boldsymbol{p}|_{2,\Omega} + h^{2+\min(\frac{1}{2},\alpha,\frac{\beta}{2})} \big(|\boldsymbol{p}|_{2,\infty,\Omega} + \|\boldsymbol{p}\|_{3,\Omega}\big). \tag{3.12}$$

By $\operatorname{div} \boldsymbol{q}_h = 0$, $\|\boldsymbol{q}_h\|_{0,\Omega} \approx 1$, (3.4) and (3.6),

$$\begin{aligned} II &= (\boldsymbol{q}_h, \boldsymbol{b}(u - u_h)) \\ &= (\boldsymbol{b} \cdot \boldsymbol{q}_h, u - P_h u + P_h u - u_h) \\ &= (\boldsymbol{b} \cdot \boldsymbol{q}_h - P_h(\boldsymbol{b} \cdot \boldsymbol{q}_h), u - P_h u) + O(h^3) \|u\|_{3,\Omega} \\ &= O(h^4) |\boldsymbol{b} \cdot \boldsymbol{q}_h|_{h,2,\Omega} |u|_{2,\Omega} + O(h^3) \|u\|_{3,\Omega}. \end{aligned} \tag{3.13}$$

Since $\boldsymbol{q}_h|_T \in \mathcal{P}_1(T)^2$, the inverse estimate implies

$$|\boldsymbol{b} \cdot \boldsymbol{q}_h|_{2,T} \lesssim \|\boldsymbol{q}_h\|_{0,T} + \|D^1 \boldsymbol{q}_h\|_{0,T} \lesssim h_T^{-1} \|\boldsymbol{q}_h\|_{0,T}.$$

(3.13) then reduces to

$$II = O(h^3) \|u\|_{3,\Omega}. \tag{3.14}$$

Then the theorem follows from (3.10)–(3.12), and (3.14). □

4 Superconvergent recovery

In this section, we introduce a new recovery operator $R_h^r : \mathcal{Q}_h^r \to \mathcal{W}_h^{r+1} \times \mathcal{W}_h^{r+1}$. For $\boldsymbol{q}_h \in \mathcal{Q}_h^r$, it suffices to specify nodal values of $R_h^r \boldsymbol{q}_h$. Here a node is the location of the degree of freedom of Lagrange elements, which can be a vertex of a triangle or an interior point of an edge/ triangle. For vertices $\boldsymbol{z}_1, \boldsymbol{z}_2, \boldsymbol{z}_3 \in \mathcal{N}_h$, let $\overline{\boldsymbol{z}_1\boldsymbol{z}_2}$ denote the edge with endpoints $\boldsymbol{z}_1, \boldsymbol{z}_2$ and $\overline{\boldsymbol{z}_1\boldsymbol{z}_2\boldsymbol{z}_3}$ the triangle with vertices $\boldsymbol{z}_1, \boldsymbol{z}_2, \boldsymbol{z}_3$. R_h^r is defined in three steps.

Step 1. For each vertex $\boldsymbol{z} \in \mathcal{N}_h$, let $R_h^r \boldsymbol{q}_h(\boldsymbol{z}) := \boldsymbol{q}_z(\boldsymbol{z})$, where $\boldsymbol{q}_z \in \mathcal{P}_{r+1}(\omega_z)^2$ minimizes the quadratic functional

$$\begin{aligned}\mathcal{F}(\boldsymbol{q}) = &\sum_{e\in\mathcal{E}_h(\omega_z)} \sum_{j=1}^{r+1} \big(\mathcal{N}_e^j(\boldsymbol{q}) - \mathcal{N}_e^j(\boldsymbol{q}_h)\big)^2 \\ &+ \sum_{T\in\mathcal{T}_h(\omega_z)} \sum_{l=1}^{r(r+1)/2} \sum_{m=1}^{2} \big(\mathcal{N}_T^{lm}(\boldsymbol{q}) - \mathcal{N}_T^{lm}(\boldsymbol{q}_h)\big)^2,\end{aligned}$$

subject to $\boldsymbol{q} \in \mathcal{P}_{r+1}(\omega_z)^2$.

Step 2. For each node $\boldsymbol{z}$ in the interior of an edge $e = \overline{\boldsymbol{z}_1\boldsymbol{z}_2} \in \mathcal{E}_h$, let

$$R_h^r \boldsymbol{q}_h(\boldsymbol{z}) := (1-\alpha)\boldsymbol{q}_{z_1}(\boldsymbol{z}) + \alpha \boldsymbol{q}_{z_2}(\boldsymbol{z}), \quad \alpha = |\boldsymbol{z} - \boldsymbol{z}_1|/|e|.$$

Step 3. For each node $\boldsymbol{z}$ in the interior of the triangle $T = \overline{\boldsymbol{z}_1\boldsymbol{z}_2\boldsymbol{z}_3} \in \mathcal{T}_h$, let

$$R_h^r \boldsymbol{q}_h(\boldsymbol{z}) := \alpha_1 \boldsymbol{q}_{z_1}(\boldsymbol{z}) + \alpha_2 \boldsymbol{q}_{z_2}(\boldsymbol{z}) + \alpha_3 \boldsymbol{q}_{z_3}(\boldsymbol{z}),$$

where $\alpha_1, \alpha_2, \alpha_3$ are barycentric coordinates of $\boldsymbol{z}$ w.r.t. $\boldsymbol{z}_1, \boldsymbol{z}_2$, and $\boldsymbol{z}_3$.

In some cases, ω_z needs be enlarged to ensure that the above LS problem has a unique solution. Since R_h^r depends only on the degrees of freedom of the RT_r element, $R_h^r \boldsymbol{q}$ is well-defined for all $\boldsymbol{q} \in \mathcal{Q}$ and $R_h^r \Pi_h^r \boldsymbol{q} = R_h^r \boldsymbol{q}$. Recall that $\mathcal{N}_e^j(\boldsymbol{q}) = \boldsymbol{q}(\boldsymbol{g}_j) \cdot \boldsymbol{n}_e$ if $\boldsymbol{q} \in \mathcal{P}_{r+1}(T)^2$ and $e \in \mathcal{E}_h(T)$.

To clarify the recovery procedure, we give details to two important cases: RT_0 and RT_1 elements.

Example 1. RT_0 *elements on triangular meshes.* In this case, $R_h^0 \boldsymbol{q}_h$ is a continuous piecewise linear function. At step 1, let $\{e_j\}_{j=1}^J = \mathcal{E}_h(\omega_z)$. Let $\boldsymbol{m}_j = (m_{j1}, m_{j2})^\intercal$ be the midpoint of e_j and $\boldsymbol{n}_j = (n_{j1}, n_{j2})^\intercal$ be a unit normal to e_j. Then $\boldsymbol{q}_z = (c_1 + c_2 x_1 + c_3 x_2, c_4 + c_5 x_1 + c_6 x_2)^\intercal \in \mathcal{P}_1(\omega_z)^2$ is the minimizer of

$$\mathcal{F}(\boldsymbol{q}) = \sum_{j=1}^{J} \big(\boldsymbol{q}(\boldsymbol{m}_j)\cdot\boldsymbol{n}_j - \boldsymbol{q}_h(\boldsymbol{m}_j)\cdot\boldsymbol{n}_j\big)^2,$$

subject to $\boldsymbol{q} \in \mathcal{P}_1(\omega_z)^2$.

Equivalently, $\boldsymbol{c}_z = (c_1, \ldots, c_6)^\intercal$ satisfies the normal equation $\boldsymbol{A}_z^\intercal \boldsymbol{A}_z \boldsymbol{c}_z = \boldsymbol{A}_z^\intercal \boldsymbol{d}_z$, where $\boldsymbol{d}_z = (\boldsymbol{q}_h(\boldsymbol{m}_1)\cdot\boldsymbol{n}_1, \ldots, \boldsymbol{q}_h(\boldsymbol{m}_J)\cdot\boldsymbol{n}_J)^\intercal$, $\boldsymbol{A}_z = (\boldsymbol{a}_1^\intercal, \ldots, \boldsymbol{a}_J^\intercal)^\intercal$ is an $N \times 6$ matrix, $\boldsymbol{a}_j = (n_{j1}, m_{j1}n_{j1}, m_{j2}n_{j1}, n_{j2}, m_{j1}n_{j2}, m_{j2}n_{j2})$. Then $R_h \boldsymbol{q}_h(\boldsymbol{z}) = \boldsymbol{q}_z(\boldsymbol{z})$ for $\boldsymbol{z} \in \mathcal{N}_h$.

To avoid ill-conditioned $\boldsymbol{A}_z$ on graded meshes, we calculate $\boldsymbol{q}_z$ by scaling it properly. Let $h_z = |\omega_z|^{\frac{1}{2}}$ and $\hat{\boldsymbol{q}}_z(\hat{\boldsymbol{x}}) = \boldsymbol{q}_z(\boldsymbol{z} + h_z\hat{\boldsymbol{x}}) = (\hat{c}_1 + \hat{c}_2\hat{x}_1 + \hat{c}_3\hat{x}_2, \hat{c}_4 + \hat{c}_5\hat{x}_1 + \hat{c}_6\hat{x}_2)^\intercal$. Then $\hat{\boldsymbol{c}}_z = (\hat{c}_1, \ldots, \hat{c}_6)^\intercal$ solves $\hat{\boldsymbol{A}}_z^\intercal\hat{\boldsymbol{A}}_z\hat{\boldsymbol{c}}_z = \hat{\boldsymbol{A}}_z^\intercal\boldsymbol{d}_z$, where $\hat{\boldsymbol{A}}_z = (\hat{\boldsymbol{a}}_1^\intercal, \ldots, \hat{\boldsymbol{a}}_J^\intercal)^\intercal$, $\hat{\boldsymbol{a}}_j = (n_{j1}, \hat{m}_{j1}n_{j1}, \hat{m}_{j2}n_{j1}, n_{j2}, \hat{m}_{j1}n_{j2}, \hat{m}_{j2}n_{j2})$, $\hat{\boldsymbol{m}}_j = (\boldsymbol{m}_j - \boldsymbol{z})/h_z = (\hat{m}_{j1}, \hat{m}_{j2})$. Then $R_h^0\boldsymbol{q}_h(\boldsymbol{z}) = (\hat{c}_1, \hat{c}_4)^\intercal$.

Example 2. *RT_1 elements on triangular meshes.* In this case, $R_h^1\boldsymbol{q}_h$ is a continuous piecewise quadratic function. At step 1, let $\{e_j\}_{j=1}^J = \mathcal{E}_h(\omega_z)$ and $\{T_l\}_{l=1}^L = \mathcal{T}_h(\omega_z)$. Let

$$\boldsymbol{q}_z = \begin{pmatrix} c_1 + c_2x_1 + c_3x_2 + c_4x_1^2 + c_5x_1x_2 + c_6x_2^2 \\ c_7 + c_8x_1 + c_9x_2 + c_{10}x_1^2 + c_{11}x_1x_2 + c_{12}x_2^2 \end{pmatrix} \in \mathcal{P}_2(\omega_z)^2$$

minimize

$$\begin{aligned}\mathcal{F}(\boldsymbol{q}) = &\sum_{j=1}^J \big(\boldsymbol{q}(\boldsymbol{x}_j)\cdot\boldsymbol{n}_j - \boldsymbol{q}_h(\boldsymbol{x}_j)\cdot\boldsymbol{n}_j\big)^2 + \big(\boldsymbol{q}(\boldsymbol{y}_j)\cdot\boldsymbol{n}_j - \boldsymbol{q}_h(\boldsymbol{y}_j)\cdot\boldsymbol{n}_j\big)^2 \\ &+ \sum_{l=1}^L\sum_{m=1}^2 \left(\frac{1}{|T_l|}\int_{T_l} q_m - \frac{1}{|T_l|}\int_{T_l} q_{h,m}\right)^2, \quad \boldsymbol{q} \in \mathcal{P}_2(\omega_z)^2,\end{aligned}$$

where $\boldsymbol{q} = (q_1, q_2)^\intercal, \boldsymbol{q}_h = (q_{h,1}, q_{h,2})^\intercal$, $\boldsymbol{x}_j = \frac{3+\sqrt{3}}{6}\boldsymbol{a}_j + \frac{3-\sqrt{3}}{6}\boldsymbol{b}_j$, $\boldsymbol{y}_j = \frac{3-\sqrt{3}}{6}\boldsymbol{a}_j + \frac{3+\sqrt{3}}{6}\boldsymbol{b}_j$, and $e_j = \overline{\boldsymbol{a}_j\boldsymbol{b}_j}$. Equivalently, $\boldsymbol{c}_z = (c_1, \ldots, c_{12})^\intercal$ solves the normal equation $\boldsymbol{A}_z^\intercal\boldsymbol{A}_z\boldsymbol{c}_z = \boldsymbol{A}_z^\intercal\boldsymbol{d}_z$, where

$$\begin{aligned}\boldsymbol{d}_z = (&\boldsymbol{q}_h(\boldsymbol{x}_1)\cdot\boldsymbol{n}_1, \boldsymbol{q}_h(\boldsymbol{y}_1)\cdot\boldsymbol{n}_1, \boldsymbol{q}_h(\boldsymbol{x}_2)\cdot\boldsymbol{n}_2, \boldsymbol{q}_h(\boldsymbol{y}_2)\cdot\boldsymbol{n}_2, \ldots, \\ &\boldsymbol{q}_h(\boldsymbol{y}_J)\cdot\boldsymbol{n}_J, \frac{1}{|T_1|}\int_{T_1} q_{h,1}, \frac{1}{|T_1|}\int_{T_1} q_{h,2}, \ldots, \frac{1}{|T_L|}\int_{T_L} q_{h,2}\bigg)^\intercal,\end{aligned}$$

and $\boldsymbol{A}_z = (\boldsymbol{a}_1^\intercal, \ldots, \boldsymbol{a}_{2J+2L}^\intercal)^\intercal$ is a $(2J+2L)\times 12$ matrix,

$$\begin{aligned}&\boldsymbol{a}_{2j-1} = (n_{j1}\boldsymbol{\xi}_j, n_{j2}\boldsymbol{\xi}_j), \quad \boldsymbol{a}_{2j} = (n_{j1}\boldsymbol{\eta}_j, n_{j2}\boldsymbol{\eta}_j), \\ &\boldsymbol{\xi}_j = (1, x_{j1}, x_{j2}, x_{j1}^2, x_{j1}x_{j2}, x_{j2}^2), \\ &\boldsymbol{\eta}_j = (1, y_{j1}, y_{j2}, y_{j1}^2, y_{j1}y_{j2}, y_{j2}^2), \quad 1 \le j \le J, \\ &\boldsymbol{a}_{2N+2l-1} = \frac{1}{|T_l|}\int_{T_l}(1, x_1, x_2, x_1^2, x_1x_2, x_2^2, 0, 0, 0, 0, 0, 0), \\ &\boldsymbol{a}_{2N+2l} = \frac{1}{|T_l|}\int_{T_l}(0, 0, 0, 0, 0, 0, 1, x_1, x_2, x_1^2, x_1x_2, x_2^2), \quad 1 \le l \le L.\end{aligned}$$

Then $R_h^1\boldsymbol{q}_h(\boldsymbol{z}) = \boldsymbol{q}_z(\boldsymbol{z})$ for $\boldsymbol{z} \in \mathcal{N}_h$. At step 2, for the midpoint $\boldsymbol{z}$ of the edge $e = \overline{\boldsymbol{z}_1\boldsymbol{z}_2}$, $R_h\boldsymbol{q}_h(\boldsymbol{z}) = (\boldsymbol{q}_{z_1}(\boldsymbol{z}) + \boldsymbol{q}_{z_2}(\boldsymbol{z}))/2$. one can again introduce the scaled polynomial $\hat{\boldsymbol{q}}_z(\hat{\boldsymbol{x}}) = \boldsymbol{q}_z(\boldsymbol{z} + h_z\hat{\boldsymbol{x}})$ in practice.

Assume that the solution of each local LS problem at each vertex $\boldsymbol{z}$ is unique. By definition R_h^r preserves $(r+1)$-degree polynomials, namely, $R_h^r\boldsymbol{q} = \boldsymbol{q}$ on T for $\boldsymbol{q} \in \mathcal{P}_{r+1}(\omega_T)^2$, which leads to the super-approximation property $\|\boldsymbol{q} - R_h^r\boldsymbol{q}\|_{0,\Omega} = O(h^{r+2})$. However, it's not obvious that these local LS problems are uniquely solvable. The next obvious lemma gives several statements equivalent to uniqueness.

Lemma 4.1 *The following statements are equivalent:*

1. *There exists a unique $\boldsymbol{q}_z$ at $\boldsymbol{z}$.*
2. *$A_z\boldsymbol{c} = \boldsymbol{0}$ implies $\boldsymbol{c} = \boldsymbol{0}$.*
3. *$\Pi_h^r \boldsymbol{q}_z = 0$ on ω_z implies $\boldsymbol{q}_z \equiv 0$.*

Hence it suffices to study the unisolvence of Π_h^r on $\mathcal{P}_{r+1}(\omega_z)^2$. Π_h^r is moment-based interpolation while nodal interpolation is often easier to analyze. The next lemma reduces Statement 3 in Lemma 4.1 to the case of Lagrange interpolation.

Lemma 4.2 *Assume $\Pi_h^r \boldsymbol{q}_z = 0$ on ω_z. Then $\boldsymbol{q}_z = \nabla^\perp w$ for some $w \in \mathcal{P}_{r+2}(\omega_z)$. In addition, for $e \in \mathcal{E}_h(\omega_z)$, $w(\boldsymbol{l}) = 0$ at any Lobatto quadrature point $\boldsymbol{l}$ on e.*

Proof $\Pi_h^r \boldsymbol{q}_z = 0$ and (2.4) imply

$$\operatorname{div} \boldsymbol{q}_z = \operatorname{div}(\boldsymbol{q}_z - \Pi_h^r \boldsymbol{q}_z) = \operatorname{div} \boldsymbol{q}_z - P_h^r \operatorname{div} \boldsymbol{q}_z = 0.$$

Hence $\boldsymbol{q}_z = \nabla^\perp w$ for some $w \in \mathcal{P}_{r+2}(\omega_z)$. Given $e = \overline{\boldsymbol{ab}} \in \mathcal{E}_h(\omega_z)$,

$$w(\boldsymbol{b}) - w(\boldsymbol{a}) = \int_e \partial_{\boldsymbol{t}_e} w = \int_e \boldsymbol{q}_z \cdot \boldsymbol{n}_e = \int_e \Pi_h^r \boldsymbol{q}_z \cdot \boldsymbol{n}_e = 0.$$

Hence $w(\boldsymbol{z}) \equiv c$ for all vertices $\boldsymbol{z}$ in ω_z. By subtracting c from w, we can assume that w vanishes at all vertices. For $v \in \mathcal{P}_r(e)$,

$$\int_e w \partial_{\boldsymbol{t}_e} v = -\int_e v \partial_{\boldsymbol{t}_e} w = -\int_e \boldsymbol{q}_z \cdot \boldsymbol{n}_e v = -\int_e \Pi_h^r \boldsymbol{q}_z \cdot \boldsymbol{n}_e v = 0,$$

and thus

$$\int_e w\tilde{v} = 0 \quad \text{for all } \tilde{v} \in \mathcal{P}_{r-1}(e). \tag{4.1}$$

Note that on $e = \overline{\boldsymbol{ab}}$, the Lobatto quadrature $\int_e f = \sum_{j=1}^{r+2} \mu_j f(\boldsymbol{l}_j)$ is exact for $f \in \mathcal{P}_{2r+1}(e)$, where $\boldsymbol{l}_j = \boldsymbol{a} + (\boldsymbol{b} - \boldsymbol{a})\hat{l}_j$, $\{\hat{l}_j\}_{j=1}^{r+2}$ are zeros of the polynomial $\frac{d^r}{ds^r}\left(s^{r+1}(1-s)^{r+1}\right)$ and $\{\mu_j\}_{j=1}^{r+2}$ are corresponding weights. Let $\tilde{v}$ be the polynomial which is μ_j^{-1} at $\boldsymbol{l}_j$ and 0 at rest of the $(r-1)$ interior quadrature points $\{\boldsymbol{l}_i\}_{i=2, i\neq j}^{r+1}$ in (4.1). Then $w(\boldsymbol{l}_j) = \int_e w\tilde{v} = 0$. The proof is complete. □

The next theorem gives practical criteria of checking the well-posedness of R_h^0 and R_h^1.

Theorem 4.1 *Let $\boldsymbol{z}$ be a vertex in $\mathcal{T}_h$. If $\#\mathcal{T}(\omega_z) \geq 5$ and the sum of each pair of adjacent angles in ω_z is $\leq \pi$, then there exists a unique $\boldsymbol{q}_z$ at $\boldsymbol{z}$ for R_h^0. If $\#\mathcal{T}(\omega_z) \geq 4$, then there exists a unique $\boldsymbol{q}_z$ at $\boldsymbol{z}$ for R_h^1.*

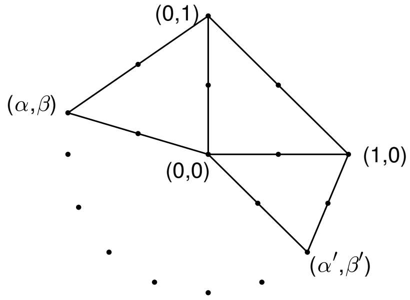

Fig. 2 A local patch containing the reference triangle.

Proof Assume $\Pi_h^r \boldsymbol{q}_z = 0$ on ω_z. By Lemma 4.2, $\boldsymbol{q}_z = \nabla^\perp w$ for some $w \in \mathcal{P}_{r+2}(\omega_z)$. If $r = 0$, then $w \in \mathcal{P}_2(\omega_z)$ vanishes at all vertices in ω_z and thus $w = 0$ by Theorem 2.3 in [22]. Hence $\boldsymbol{q}_z = \mathbf{0}$.

If $r = 1$, $w \in \mathcal{P}_3(\omega_z)$ vanishes at all vertices and midpoints of edges in ω_z. Without loss of generality, we can assume that $\boldsymbol{z} = (0,0)$ and the reference triangle $\hat{T}$ spanned by $(0,0), (0,1), (1,0)$ is in $\mathcal{T}_h(\omega_z)$.

If w is reducible, then the zero set $w^{-1}(0)$ is the union of three straight lines(counting multiplicity) or the union of a straight line and a conic. Clearly three lines cannot pass all vertices and midpoints in ω_z provided $\#\mathcal{T}_h(\omega_z) \geq 4$. If $w^{-1}(0)$ contains a conic branch C, then C must contain at least two vertices $\boldsymbol{a}, \boldsymbol{b}$ in ω_z because $\#\mathcal{T}_h(\omega_z) \geq 4$. However, C cannot pass through $(\boldsymbol{a}+\boldsymbol{b})/2$ by elementary geometry.

Hence reducible w cannot vanish at all nodes in ω_z and we can assume

$$w = c_1 x_1^3 + c_2 x_1^2 x_2 + c_3 x_1 x_2^2 + c_4 x_2^3 + c_5 x_2^2 + c_6 x_1 x_2 + c_7 x_2^2 + c_8 x_1 + c_9 x_2$$

is irreducible. Furthermore, we can assume one of the coefficients of highest order terms is 1, say $c_1 = 1$(similar argument for c_2, c_3 or $c_4 = 1$). Let (α, β) be the vertex outside $\hat{T}$ next to $(0,1)$, see Figure 2. Solving the linear system of equations

$$\begin{aligned} &w(1,0) = w(0,1) = w(1/2,0) = w(0,1/2) = w(1/2,1/2) \\ &= w(\alpha,\beta) = w\left(\frac{\alpha}{2}, \frac{\beta+1}{2}\right) = w\left(\frac{\alpha}{2}, \frac{\beta}{2}\right) = 0, \end{aligned}$$

we have

$$c_1 = \frac{3-3\alpha}{1+\beta}, \quad c_2 = \frac{3\alpha(\alpha-1)}{\beta(1+\beta)}. \tag{4.2}$$

Note that $\beta \neq 0, \beta \neq -1$ in (4.2), otherwise the irreducible cubic curve $w^{-1}(0)$ intersects with a line at five distinct points, which is impossible by Bézout's theorem (cf.[25]). Also $\alpha \neq 1$ otherwise it violates the topology of the patch ω_z. Hence $\alpha/\beta = -c_2/c_1$. Let (α', β') be the vertex outside $\hat{T}$ next to $(1,0)$.

Similarly we have $\alpha'/\beta' = -c_2/c_1$. Then it forces $(\alpha,\beta) = (\alpha',\beta')$, which contradicts $\#\mathcal{T}_h(\omega_z) \geq 4$. Hence $r \equiv 0$ and $\boldsymbol{q}_z \equiv 0$.

Therefore by Lemma 4.1, there exists a unique $\boldsymbol{q}_z$ for $r = 0, 1$. □

We say a vertex $\boldsymbol{z}$ is good if the condition in Theorem 4.1 holds at $\boldsymbol{z}$, otherwise it is a bad vertex. In practice, $\mathcal{T}_h$ typically has a few bad vertices, e.g., boundary vertices. There are several ways of dealing with a bad vertex $\boldsymbol{z}$. If $\boldsymbol{z}$ is directly connected to a good vertex $\boldsymbol{z}'$, one can define $\omega_z := \omega_{z'}$ and thus $\boldsymbol{A}_z$ is of full column rank. A more convenient way is to *empirically* add some extra elements to the patch ω_z in practice, e.g., enlarge ω_z by one layer. Alternatively, one can solve a rank-deficient local least squares problem, which might reduce the rate of superconvergence of R_h.

In the rest of this paper, we assume that

At each vertex $\boldsymbol{z}$, there exists a unique $\boldsymbol{q}_z$.

Using the uniqueness of the LS solution, we obtain the boundedness of R_h^r.

Theorem 4.2 *For $\boldsymbol{q}_h \in \mathcal{Q}_h^r$ and $T \in \mathcal{T}_h$,*

$$\|R_h^r \boldsymbol{q}\|_{0,T} \lesssim \|\boldsymbol{q}\|_{0,\omega_T}, \quad r = 0, 1.$$

Proof For $\boldsymbol{z} \in \mathcal{N}_h$, Let $\sigma_{\min}$ and $\sigma_{\max}$ be the minimum and maximum singular values of $\hat{\boldsymbol{A}}_z$ respectively. The goal is to show that $\sigma_{\min}$ is uniformly bounded away from 0. MAC implies $\#\mathcal{T}_h(\omega_z) \leq N_{\max} = 2\pi/\Theta$. Hence it suffices to consider the case $\#\mathcal{T}_h(\omega_z) = N$ for some fixed $N \leq N_{\max}$. In this case, $\#\mathcal{E}_h(\omega_z) = 2N$. Let $N_1 = 2N, N_2 = 6$ provided $k = 0$ and $N_1 = 6N, N_2 = 12$ provided $k = 1$. Let $M_{N_1\times N_2}$ and $S_{N_1\times N_2}$ be the set of $N_1 \times N_2$ matrices and $N_1 \times N_2$ rank-deficient matrices, respectively. It is well known that $\sigma_{\min} = \mathrm{dist}(\hat{\boldsymbol{A}}_z, S_{N_1\times N_2})$, the distance (measured by matrix 2-norm) from $\hat{\boldsymbol{A}}_z$ to rank-deficient matrices. $\mathrm{dist}(\cdot, S_{N_1\times N_2})$ is continuous on $M_{N_1\times N_2}$. Recall that $\hat{\boldsymbol{A}}_z$ is the scaled LS coefficient matrix determined by ω_z. Consider all possible ω_z and define

$$\mathcal{A}_z = \{\hat{\boldsymbol{A}}_z \in M_{N_1\times N_2} : \#\mathcal{T}_h(\omega_z) = N, \omega_z \text{ satisfies MAC}\}.$$

Clearly $\mathcal{A}_z$ is a compact set in $M_{N_1\times N_2}$ and any $\hat{\boldsymbol{A}}_z \in \mathcal{A}_z$ is of full rank by the uniqueness assumption. Hence $\sigma_{\min} = \mathrm{dist}(\hat{\boldsymbol{A}}_z, S_{N_1\times N_2}) \geq C_1 > 0$, where C_1 depends only on the minimum angle Θ. The maximum singular value $\sigma_{\max} \leq C_2$, where C_2 only depends on Ω. For $\boldsymbol{q}_h \in \mathcal{Q}_h^r$,

$$\begin{aligned} |\hat{\boldsymbol{c}}_z| &\leq \|(\hat{\boldsymbol{A}}_z^\intercal \hat{\boldsymbol{A}}_z)^{-1}\|_2 |\hat{\boldsymbol{A}}_z^\intercal \boldsymbol{d}_z| \leq \sigma_{\min}^{-2}\sigma_{\max}|\boldsymbol{d}_z| \\ &\leq C_1^{-2} C_2 \|\boldsymbol{q}_h\|_{0,\infty,\omega_z} \lesssim h_z^{-1}\|\boldsymbol{q}_h\|_{0,\omega_z}, \end{aligned} \tag{4.3}$$

where $|\cdot|$ is the Euclidean norm. Finally by (4.3), we have

$$\|R_h^r \boldsymbol{q}_h\|_{0,T} \lesssim h\|R_h^r \boldsymbol{q}_h\|_{0,\infty,T} \lesssim h|\hat{\boldsymbol{c}}_z| \lesssim \|\boldsymbol{q}_h\|_{0,\omega_T},$$

which completes the proof. □

The super-approximation property of R_h follows from the uniqueness and boundedness results.

Theorem 4.3 *For $\boldsymbol{q} \in H^{r+2}(\Omega)$,*

$$\|\boldsymbol{q} - R_h^r \boldsymbol{q}\|_{0,\Omega} \lesssim h^{r+2} |\boldsymbol{q}|_{r+2,\Omega}, \quad r = 0, 1.$$

Proof Let $T = \overline{\boldsymbol{z}_1\boldsymbol{z}_2\boldsymbol{z}_3} \in \mathcal{T}_h$ and $T_1 \subset \overline{\Omega}$ be a smallest local triangle containing ω_T. Let $\boldsymbol{q}_{r+1} \in \mathcal{P}_{r+1}(T_1)^2$ be the degree-$(r+1)$ local Lagrange interpolant of $\boldsymbol{q}$ using based on T_1. By the uniqueness assumption, $R_h^r \boldsymbol{q}_{r+1} = \boldsymbol{q}_{r+1}$ on T. It then follows from $R_h^r \Pi_h^r = R_h^r$ that

$$\|\boldsymbol{q} - R_h^r \boldsymbol{q}\|_{0,T} \leq \|\boldsymbol{q} - \boldsymbol{q}_{r+1}\|_{0,T} + \|R_h^r \Pi_h^r (\boldsymbol{q}_{r+1} - \boldsymbol{q})\|_{0,T}. \tag{4.4}$$

Using the boundedness from Theorem 4.2, the stability in (2.3), and (1.6),

$$\begin{aligned}\|R_h^r \Pi_h^r (\boldsymbol{q}_{r+1} - \boldsymbol{q})\|_{0,T} &\lesssim \|\Pi_h^r (\boldsymbol{q}_{r+1} - \boldsymbol{q})\|_{0,\omega_T} \\ &\lesssim h \|\Pi_h^r (\boldsymbol{q}_{r+1} - \boldsymbol{q})\|_{0,\infty,\omega_T} \lesssim h \|\boldsymbol{q}_{r+1} - \boldsymbol{q}\|_{0,\infty,\omega_T} \lesssim h^{r+2} |\boldsymbol{q}|_{r+2,T_1}.\end{aligned} \tag{4.5}$$

Combining (4.4), (4.5) and the shape regularity $\mathcal{T}_h$ completes the proof. □

In the end, we present the superconvergent recovery estimate.

Theorem 4.4 *Assume that $\mathcal{T}_h$ satisfies the (α, β)-condition. Then*

$$\|\boldsymbol{p} - R_h^r \boldsymbol{p}_h^r\|_{0,\Omega} \lesssim h^{r+1+\min(\frac{1}{2}, \alpha, \frac{\beta}{2})} \big(|\boldsymbol{p}|_{r+1,\infty,\Omega} + \|\boldsymbol{p}\|_{r+2,\Omega} \big), \quad r = 0, 1.$$

Proof The theorem follows from

$$\|\boldsymbol{p} - R_h^r \boldsymbol{p}_h^r\|_{0,\Omega} \leq \|\boldsymbol{p} - R_h^r \boldsymbol{p}\|_{0,\Omega} + \|R_h^r (\Pi_h^r \boldsymbol{p} - \boldsymbol{p}_h^r)\|_{0,\Omega},$$

Theorems 4.2 and 4.3, Theorem 3.2($r = 1$) or Theorem 4.5($r = 0$) in [19]. □

5 Proof of Lemma 2.1

The following elementary triangular identities hold:

$$\begin{aligned}
&\cos\theta_k = (\ell_{k-1}^2 + \ell_{k+1}^2 - \ell_k^2)/(2\ell_{k-1}\ell_{k+1}), \quad \sin\theta_k = \ell_k/d, \quad d_k = \ell_{k-1}\ell_{k+1}/d, \\
&\boldsymbol{n}_{k-1} = -\sin\theta_{k+1}\boldsymbol{t}_k - \cos\theta_{k+1}\boldsymbol{n}_k, \quad \boldsymbol{n}_{k+1} = \sin\theta_{k-1}\boldsymbol{t}_k - \cos\theta_{k-1}\boldsymbol{n}_k, \\
&\partial_{\boldsymbol{t}_{k-1}}^2 = \cos^2\theta_{k+1}\partial_{\boldsymbol{t}_k}^2 - 2\cos\theta_{k+1}\sin\theta_{k+1}\partial_{\boldsymbol{t}_k\boldsymbol{n}_k}^2 + \sin^2\theta_{k+1}\partial_{\boldsymbol{n}_k}^2, \\
&\partial_{\boldsymbol{t}_{k+1}}^2 = \cos^2\theta_{k-1}\partial_{\boldsymbol{t}_k}^2 + 2\cos\theta_{k-1}\sin\theta_{k-1}\partial_{\boldsymbol{t}_k\boldsymbol{n}_k}^2 + \sin^2\theta_{k-1}\partial_{\boldsymbol{n}_k}^2.
\end{aligned} \tag{5.1}$$

For each edge e_k, we define several associated geometric quantities $\{\alpha_{jl,k}^i\}_{1\leq i,j,l\leq 2}$

$$\begin{aligned}
&\alpha_{11,k}^1 = \frac{1}{24d\ell_k^2}\ell_{k-1}\ell_{k+1}\big(3\ell_k^4 - (\ell_{k-1}^2 - \ell_{k+1}^2)^2\big), \\
&\alpha_{12,k}^1 = \alpha_{21,k}^1 = \frac{1}{12d^2\ell_k}\ell_{k-1}^2\ell_{k+1}^2(\ell_{k-1}^2 - \ell_{k+1}^2), \quad \alpha_{22,k}^1 = -\frac{1}{6d^3}\ell_{k+1}^3\ell_{k-1}^3, \\
&\alpha_{11,k}^2 = \frac{1}{48\ell_k^3}(\ell_{k-1}^2 - \ell_{k+1}^2)\big(9\ell_k^4 - (\ell_{k-1}^2 - \ell_{k+1}^2)^2\big), \\
&\alpha_{12,k}^2 = \alpha_{21,k}^2 = -\alpha_{11,k}^1, \quad \alpha_{22,k}^2 = -\alpha_{12,k}^1.
\end{aligned}$$

To prove Lemma 2.1, we introduce cubic bubble functions

$$\psi_0 = \lambda_1\lambda_2\lambda_3, \quad \psi_k = \lambda_{k-1}\lambda_{k+1}(\lambda_{k-1} - \lambda_{k+1}), \quad 1 \le k \le 3.$$

By counting the dimension, it is clear that $\{\psi_k\}_{k=0}^3$ can span polynomials in $\mathcal{P}_3(T)$ that vanish at $\{\boldsymbol{z}_k\}_{k=1}^3$ and midpoints of $\{e_k\}_{k=1}^3$. In fact, $\{\psi_k\}_{k=0}^3$ has been used to derive superconvergence of quadratic Lagrange elements (cf.[15]) and a posteriori error estimators (cf.[5]).

Lemma 5.1 *For $\boldsymbol{p}_2 \in \mathcal{P}_2(T)^2$,*

$$\boldsymbol{p}_2 - \Pi_h^1 \boldsymbol{p}_2 = \nabla^\perp r,$$

where

$$r = \alpha^i_{jl,\beta}\mathcal{D}^{jl}_{i,\beta}(\boldsymbol{p}_2)\psi_0 + \sum_{k=1}^3 \frac{\ell_k^3}{12}\mathcal{D}^{11}_{2,k}(\boldsymbol{p}_2)\psi_k, \quad \forall 1 \le \beta \le 3.$$

Proof By $\Pi_h^1(\boldsymbol{p}_2 - \Pi_h^1\boldsymbol{p}_2) = 0$ and using Lemma 4.2, we have

$$\boldsymbol{p}_2 - \Pi_h^1 \boldsymbol{p}_2 = \nabla^\perp \big(\sum_{k=0}^3 c_k\psi_k\big). \tag{5.2}$$

For a unit vector $\boldsymbol{d}$ and the directional derivative $\partial_{\boldsymbol{d}}$, the definition of $\mathcal{RT}_1(T)$ implies that $\partial^2_{\boldsymbol{d}}\Pi_h^1\boldsymbol{p}_2$ is proportional to $\boldsymbol{d}$. Then applying $\boldsymbol{d}^\perp \cdot \partial^2_{\boldsymbol{d}}$ to (5.2) gives

$$\boldsymbol{d}^\perp \cdot \partial^2_{\boldsymbol{d}}\boldsymbol{p}_2 = \sum_{k=0}^3 c_k \partial^3_{\boldsymbol{d}}\psi_k. \tag{5.3}$$

By direct calculation,

$$\partial^3_{\boldsymbol{d}}\psi_0 = 6\partial_{\boldsymbol{d}}\lambda_1\partial_{\boldsymbol{d}}\lambda_2\partial_{\boldsymbol{d}}\lambda_3, \tag{5.4a}$$

$$\partial^3_{\boldsymbol{d}}\psi_k = 6\partial_{\boldsymbol{d}}\lambda_{k-1}\partial_{\boldsymbol{d}}\lambda_{k+1}(\partial_{\boldsymbol{d}}\lambda_{k-1} - \partial_{\boldsymbol{d}}\lambda_{k+1}), \quad 1 \le k \le 3. \tag{5.4b}$$

In particular, $\partial^3_{\boldsymbol{t}_k}\psi_0 = 0$ and $\partial^3_{\boldsymbol{t}_k}\psi_j = -12\delta_{jk}/\ell_k^3$. By (5.4) and (5.3) with $\boldsymbol{d} = \boldsymbol{t}_k$, we have

$$c_k = \frac{\ell_k^3}{12}\boldsymbol{n}_k \cdot \partial^2_{\boldsymbol{t}_k}\boldsymbol{p}_2 = \frac{\ell_k^3}{12}\mathcal{D}^{11}_{2,k}(\boldsymbol{p}_2), \quad 1 \le k \le 3. \tag{5.5}$$

It remains to determine c_0. (5.3) with $\boldsymbol{d} = \boldsymbol{n}_k$ implies that

$$\mathcal{D}^{22}_{1,k}(\boldsymbol{p}_2) = c_0\partial^3_{\boldsymbol{n}_k}\psi_0 + c_k\partial^3_{\boldsymbol{n}_k}\psi_k + c_{k-1}\partial^3_{\boldsymbol{n}_k}\psi_{k-1} + c_{k+1}\partial^3_{\boldsymbol{n}_k}\psi_{k+1}, \tag{5.6}$$

By $\partial_{\boldsymbol{n}_k}\lambda_k = -1/d_k, \partial_{\boldsymbol{n}_k}\lambda_{k+1} = \cos\theta_{k-1}/d_{k+1}, \partial_{\boldsymbol{n}_k}\lambda_{k-1} = \cos\theta_{k+1}/d_{k-1}$, (5.4) with $\boldsymbol{d} = \boldsymbol{n}_k$, (5.5), and (5.6), we obtain

$$\begin{aligned} c_0 = &-\frac{d_{k-1}d_k d_{k+1}}{6\cos\theta_{k-1}\cos\theta_{k+1}}\mathcal{D}^{22}_{1,k}(\boldsymbol{p}_2) \\ &+\frac{\ell_k^3}{12}d_k\left(\frac{\cos\theta_{k+1}}{d_{k-1}} - \frac{\cos\theta_{k-1}}{d_{k+1}}\right)\mathcal{D}^{11}_{2,k}(\boldsymbol{p}_2) \\ &-\frac{\ell_{k-1}^3}{12}\frac{d_{k-1}}{\cos\theta_{k+1}}\left(\frac{1}{d_k} + \frac{\cos\theta_{k-1}}{d_{k+1}}\right)\mathcal{D}^{11}_{2,k-1}(\boldsymbol{p}_2) \\ &+\frac{\ell_{k+1}^3}{12}\frac{d_{k+1}}{\cos\theta_{k-1}}\left(\frac{1}{d_k} + \frac{\cos\theta_{k+1}}{d_{k-1}}\right)\mathcal{D}^{11}_{2,k+1}(\boldsymbol{p}_2). \end{aligned} \tag{5.7}$$

Then using (5.1) and (5.7), we obtain $c_0 = \alpha^i_{jl,k}\mathcal{D}^{jl}_{i,k}(\boldsymbol{p}_2), 1 \le k \le 3$. □

Now we can prove Lemma 2.1. In the proof, we shall use the integral formula

$$\int_T \lambda_1^{m_1}\lambda_2^{m_2}\lambda_3^{m_3} = \frac{2|T|m_1!m_2!m_3!}{(m_1+m_2+m_3+2)!}, \quad \int_e \lambda_1^{m_1}\lambda_2^{m_2} = \frac{|e|m_1!m_2!}{(m_1+m_2+1)!}, \tag{5.8}$$

where λ_1, λ_2 are barycentric coordinates w.r.t. the edge e.

Proof Using (2.1) and Lemma 5.1, we have

$$\int_T (\boldsymbol{p}_2 - \Pi_h^1\boldsymbol{p}_2)\cdot\nabla^\perp r_2 = \sum_{k=1}^3\int_{e_k} r\nabla^\perp r_2\cdot\boldsymbol{t}_k - \int_T r\Delta r_2 := I + II. \tag{5.9}$$

Recall that $\phi_k = \lambda_{k-1}\lambda_{k+1}$ and let I_h be the linear interpolation. Then using the hierarchical representation

$$r_2 - I_h r_2 = -\frac{1}{2}\sum_{k=1}^3 \ell_k^2\phi_k\partial^2_{\boldsymbol{t}_k}r_2, \tag{5.10}$$

and $\Delta\phi_k = 2\nabla\lambda_{k-1}\cdot\nabla\lambda_{k+1} = -2\cos\theta_k/(d_{k-1}d_{k+1})$, we obtain

$$\Delta r_2 = \frac{1}{4|T|^2}\sum_{k=1}^3 \ell_k^2\ell_{k-1}\ell_{k+1}\cos\theta_k\partial^2_{\boldsymbol{t}_k}r_2. \tag{5.11}$$

It then follows from Lemma 5.1, (5.11), and $\int_T\psi_0 = |T|/60$, $\int_T\psi_k = 0, 1 \le k \le 3$, that

$$\begin{aligned} II &= -\frac{|T|}{60}c_0\Delta r_2 = -\frac{1}{240|T|}\sum_{k=1}^3 c_0\ell_k^2\ell_{k-1}\ell_{k+1}\cos\theta_k\partial^2_{\boldsymbol{t}_k}r_2 \\ &= -\frac{1}{120}\sum_{k=1}^3\int_{e_k}\alpha^i_{jl,k}\mathcal{D}^{jl}_{i,k}(\boldsymbol{p}_2)\ell_k\cot\theta_k\partial^2_{\boldsymbol{t}_k}r_2. \end{aligned} \tag{5.12}$$

By the elementary identity $\boldsymbol{t}_k = \frac{\cos\theta_{k+1}}{\sin\theta_k}\boldsymbol{n}_{k+1} - \frac{\cos\theta_{k-1}}{\sin\theta_k}\boldsymbol{n}_{k-1}$, Lemma 5.1, and $\psi_k = -\ell_k\partial_{\boldsymbol{t}_k}(\phi_k^2)/2$, we have

$$\begin{aligned}
I &= -\sum_{k=1}^{3}\frac{1}{12}\int_{e_k}\ell_k^3\mathcal{D}_{2,k}^{11}(\boldsymbol{p}_2)\psi_k\nabla^{\perp}r_2\cdot\left(\frac{\cos\theta_{k-1}}{\sin\theta_k}\boldsymbol{n}_{k-1}-\frac{\cos\theta_{k+1}}{\sin\theta_k}\boldsymbol{n}_{k+1}\right)\\
&= \sum_{k=1}^{3}\frac{1}{24}\int_{e_k}\ell_k^4\mathcal{D}_{2,k}^{11}(\boldsymbol{p}_2)\phi_k^2\left(\frac{\cos\theta_{k-1}}{\sin\theta_k}\partial^2_{\boldsymbol{t}_k\boldsymbol{t}_{k-1}}r_2-\frac{\cos\theta_{k+1}}{\sin\theta_k}\partial^2_{\boldsymbol{t}_k\boldsymbol{t}_{k+1}}r_2\right).
\end{aligned} \tag{5.13}$$

Then using the quadrature rule (5.8),

$$I = \frac{1}{720}\sum_{k=1}^{3}\ell_k^5\mathcal{D}_{2,k}^{11}(\boldsymbol{p}_2)\left(\frac{\cos\theta_{k-1}}{\sin\theta_k}\partial^2_{\boldsymbol{t}_k\boldsymbol{t}_{k-1}}r_2-\frac{\cos\theta_{k+1}}{\sin\theta_k}\partial^2_{\boldsymbol{t}_k\boldsymbol{t}_{k+1}}r_2\right).$$

In addition, (5.10) gives

$$\begin{aligned}
\partial^2_{\boldsymbol{t}_k\boldsymbol{t}_{k-1}}r_2 &= -\frac{\ell_k}{2\ell_{k-1}}\partial^2_{\boldsymbol{t}_k}r_2+\frac{\ell_{k+1}^2}{2\ell_{k-1}\ell_k}\partial^2_{\boldsymbol{t}_{k+1}}r_2-\frac{\ell_{k-1}}{2\ell_k}\partial^2_{\boldsymbol{t}_{k-1}}r_2,\\
\partial^2_{\boldsymbol{t}_k\boldsymbol{t}_{k+1}}r_2 &= -\frac{\ell_k}{2\ell_{k+1}}\partial^2_{\boldsymbol{t}_k}r_2-\frac{\ell_{k+1}}{2\ell_k}\partial^2_{\boldsymbol{t}_{k+1}}r_2+\frac{\ell_{k-1}^2}{2\ell_k\ell_{k+1}}\partial^2_{\boldsymbol{t}_{k-1}}r_2.
\end{aligned}$$

Therefore,

$$\begin{aligned}
I = \frac{1}{1440}\sum_{k=1}^{3}\int_{e_k}\Bigg\{&\frac{\ell_k^5}{\sin\theta_k}\mathcal{D}_{2,k}^{11}(\boldsymbol{p}_2)\left(\frac{\cos\theta_{k+1}}{\ell_{k+1}}-\frac{\cos\theta_{k-1}}{\ell_{k-1}}\right)\\
&+\frac{\ell_{k-1}^4}{\sin\theta_{k-1}}\mathcal{D}_{2,k-1}^{11}(\boldsymbol{p}_2)\left(\cos\theta_k+\frac{\ell_k}{\ell_{k+1}}\cos\theta_{k+1}\right)\\
&-\frac{\ell_{k+1}^4}{\sin\theta_{k+1}}\mathcal{D}_{2,k+1}^{11}(\boldsymbol{p}_2)\left(\frac{\ell_k}{\ell_{k-1}}\cos\theta_{k-1}+\cos\theta_k\right)\Bigg\}\partial^2_{\boldsymbol{t}_k}r_2
\end{aligned} \tag{5.14}$$

Combining (5.12), (5.14) and using (5.1), we obtain Lemma 2.1. □

6 Numerical experiments

We test our recovery operators R_h^r with $r = 1, 2, 3$ by the Poisson equation

$$-\Delta u = f \text{ in } \Omega,$$

where Ω and u will be given in the next three experiments. Readers are referred to [19] for numerical results on recovery superconvergence of the RT_0 element. The experiments are implemented using the iFEM package [8] in Matlab 2018b. In tables, $\|\cdot\|$ is the L^2-norm $\|\cdot\|_{0,\Omega}$, 'nt' denotes the number of triangles. The order of convergence is p such that error$\approx$ ndof$^{-\frac{p}{2}}$, where ndof is the number of degrees of freedom. The value of p is computed by least squares.

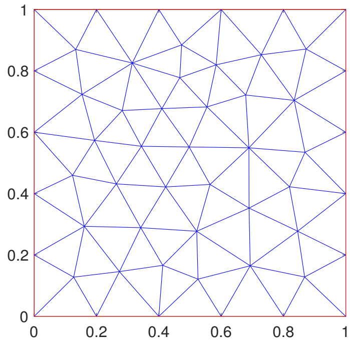

Fig. 3 Delaunay initial grid on a square.

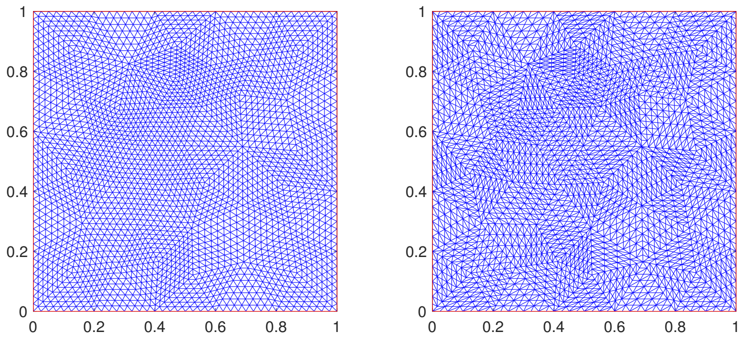

Fig. 4 (left)Regular refinement, 5504 elements. (right)Newest vertex bisection, 5504 elements.

Problem 1. In the first experiment, let Ω be the unit square $[0,1]^2$ and

$$u = \exp(x_1 + x_2)\sin(2\pi x_1)\sin(\pi x_2)$$

be the exact solution. Due to Theorem 4.1, we do not enlarge the patch ω_z when z is an interior vertex. If z is a boundary vertex, extra neighboring elements are added to ω_z such that $\#\omega_z \geq 8$. It turns out that all local least squares problems are uniquely solvable. We start with the Delaunay triangulation in Fig. 3, and computed a sequence of meshes by regular refinement, i.e., dividing an element into four similar subelements by connecting the midpoints of each edge, see Table 1. We also computed a sequence of meshes by newest vertex bisection (cf. [20,8]), see Fig. 4 and Table 2.

For regular refinement, the sequence of grids satisfies (α,β)-condition with $(\alpha,\beta) = (\infty,1)$. For RT_1 elements, Theorem 3.2 predicts that $\|\mathit{\Pi}_h^1 \boldsymbol{p} - \boldsymbol{p}_h^1\| = O(h^{2.5})$, which is confirmed by Table 1. In view of the high order recovery superconvergence $\|\boldsymbol{p} - R_h^1\boldsymbol{p}_h^1\| = O(h^{3.4})$, our supercloseness estimate $\|\boldsymbol{p} - R_h^1\boldsymbol{p}_h^1\| = O(h^{2.5})$ in Theorem 4.4 might be suboptimal.

The sequence of grids created by newest vertex bisection is far from uniformly parallel, i.e., almost no pair of adjacent triangles forms an $O(h^{1+\alpha})$ approximate parallelogram with some positive α. Hence there is no supercloseness in Table 2. Surprisingly, we still observe apparent superconvergence for $\|\boldsymbol{p} - R_h^1 \boldsymbol{p}_h^1\|$.

Problem 2: Although our supercloseness estimates only work for RT_0 and RT_1 elements, we perform numerical experiments on the recovery operators R_h^2 and R_h^3 for RT_2 and RT_3 elements. We use the same Ω, u, and initial mesh with regular refinement in Problem 1. Local patches ω_z is chosen in the same way as in Problem 1. The numerical results are presented in Tables 3 and 4.

As mentioned in Problem 1, the sequence of grids satisfies (α, β)-condition with $(\alpha, \beta) = (\infty, 1)$. Unlike RT_0 and RT_1 elements, there is no supercloseness phenomenon for RT_2 and RT_3 even on regularly refined meshes. However, it can be observed that the rate of recovery superconvergence is at least $\|\boldsymbol{p} - R_h^r \boldsymbol{p}_h^r\| = O(h^{r+2})$ with $r = 2, 3$. Therefore, the supercloseness estimate is not a necessary ingredient of superconvergence analysis. We conjecture that the superconvergence is due to a significant number of locally symmetric patches, see [24] for the theory of Lagrange elements.

Problem 3. Postprocessing superconvergence is often used to develop recovery-type a posteriori error estimator and adaptive FEMs. In the end, we test the adaptivity performance of R_h^1 on the domain $\Omega = [-1, 1]^2 \backslash \Omega_0$, where Ω_0 is a right triangle whose smallest angle is $\omega = \pi/24$, see Fig. 5(left). Let

$$u(r, \theta) = r^{\frac{\pi}{2\pi - \omega}} \sin\left(\frac{\pi}{2\pi - \omega}\theta\right) - \frac{r^2}{4},$$

where (r, θ) is the polar coordinate. The corresponding source $f = -\Delta u = 1$. We use the classical adaptive feedback loop (cf. [10,21])

$$\mathsf{SOLVE} \rightarrow \mathsf{ESTIMATE} \rightarrow \mathsf{MARK} \rightarrow \mathsf{REFINE}.$$

It will return a sequence of meshes $\{\mathcal{T}_{h_\ell}\}_{\ell \geq 0}$ and numerical solutions $\{\boldsymbol{p}_{h_\ell}\}_{\ell \geq 0}$. The algorithm starts from the initial grid $\mathcal{T}_{h_0}$ in Fig. 5(left). In the procedure ESTIMATE, $\eta_T = \|R_{h_\ell}^1 \boldsymbol{p}_{h_\ell}^1 - \boldsymbol{p}_{h_\ell}^1\|_{0,T}$ serves as a posteriori error estimator for each triangle $T \in \mathcal{T}_{h_\ell}$. The procedure MARK selects a collection of triangles $\mathcal{M}_\ell \subset \mathcal{T}_{h_\ell}$ such that

$$\sum_{T \in \mathcal{M}_\ell} \eta_T^2 \geq 0.3 \sum_{T \in \mathcal{T}_{h_\ell}} \eta_T^2.$$

Then the elements in $\mathcal{M}_\ell$ and necessary neighboring elements are refined by local mesh refinement strategy to yield a conforming subtriangulation $\mathcal{T}_{h_{\ell+1}}$ of $\mathcal{T}_{h_\ell}$. In particular, we use regular refinement with bisection closure in the procedure REFINE, see Fig. 5(right) for an adaptively refined triangulation. The numerical results are presented in Fig. 6.

It can be observed that the adaptive algorithm yields optimal rate of convergence and apparent recovery superconvergence. A distinct feature of the a posteriori error estimator $\eta_{h_\ell} := \|R^1_{h_\ell}\boldsymbol{p}^1_{h_\ell} - \boldsymbol{p}^1_{h_\ell}\|_{0,\Omega} = \big(\sum_{T\in\mathcal{T}_{h_\ell}} \eta_T^2\big)^{\frac{1}{2}}$ is the well-known asymptotic exactness:

$$\lim_{\ell\to\infty} \frac{\eta_{h_\ell}}{\|\boldsymbol{p} - \boldsymbol{p}^1_{h_\ell}\|_{0,\Omega}} = 1,$$

which is numerically confirmed using the rate of superconvergence in Fig. 6 with a triangle inequality, see, e.g., [27,4] for details.

Table 1 RT_1 with regular refinement

nt	$\|\boldsymbol{p} - \boldsymbol{p}^1_h\|$	$\|\Pi^1_h\boldsymbol{p} - \boldsymbol{p}^1_h\|$	$\|\boldsymbol{p} - R^1_h\boldsymbol{p}^1_h\|$
86	3.176e-1	4.297e-2	5.186e-1
344	8.000e-2	7.852e-3	5.560e-2
1376	2.006e-2	1.397e-3	5.344e-3
5504	5.022e-3	2.461e-4	4.929e-4
22106	1.256e-3	4.336e-5	4.616e-5
order	1.998	2.501	3.414

Table 2 RT_1 with bisection refinement

nt	$\|\boldsymbol{p} - \boldsymbol{p}^1_h\|$	$\|\Pi^1_h\boldsymbol{p} - \boldsymbol{p}^1_h\|$	$\|\boldsymbol{p} - R^1_h\boldsymbol{p}^1_h\|$
86	3.176e-1	4.297e-2	5.186e-1
344	1.325e-1	1.092e-1	7.453e-2
1376	3.401e-2	2.682e-2	1.005e-2
5504	8.604e-3	6.607e-3	1.610e-3
22016	2.164e-3	1.637e-3	3.336e-4
order	1.979	2.020	2.605

Table 3 RT_2 with regular refinement

nt	$\|\boldsymbol{p} - \boldsymbol{p}^2_h\|$	$\|\Pi^2_h\boldsymbol{p} - \boldsymbol{p}^2_h\|$	$\|\boldsymbol{p} - R^2_h\boldsymbol{p}^2_h\|$
86	2.378e-2	5.201e-3	1.505e-1
344	3.022e-3	5.488e-4	1.005e-2
1376	3.792e-4	6.501e-5	5.247e-4
5504	4.745e-5	8.002e-6	2.551e-5
22106	5.933e-6	9.953e-7	1.351e-6
order	2.993	3.080	4.215

7 Concluding remarks

In this paper, we develop supercloseness estimate for the second lowest order RT element and a family of postprocessing operators R^r_h for higher order RT elements applied to second order elliptic equations. Since both the analysis of

Table 4 RT_3 with regular refinement

nt	$\|\boldsymbol{p}-\boldsymbol{p}_h^3\|$	$\|\Pi_h^3\boldsymbol{p}-\boldsymbol{p}_h^3\|$	$\|\boldsymbol{p}-R_h^3\boldsymbol{p}_h^3\|$
86	3.733e-3	3.394e-3	4.022e-2
344	2.359e-4	2.140e-4	1.180e-3
1376	1.478e-5	1.338e-5	2.668e-5
5504	9.242e-7	8.354e-7	6.377e-7
order	3.994	3.996	5.330

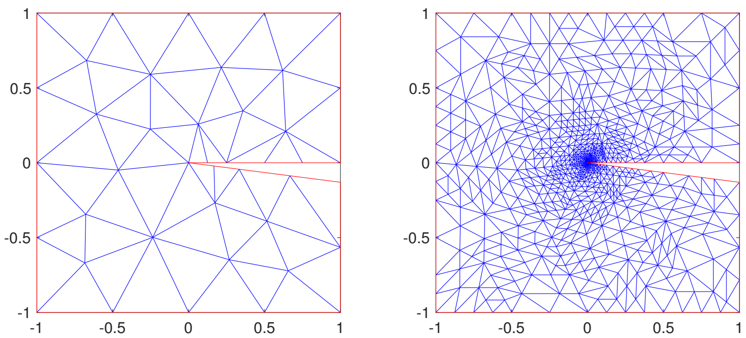

Fig. 5 (left)Initial grid for the adaptive algorithm. (right)Adaptive grid, 2026 elements.

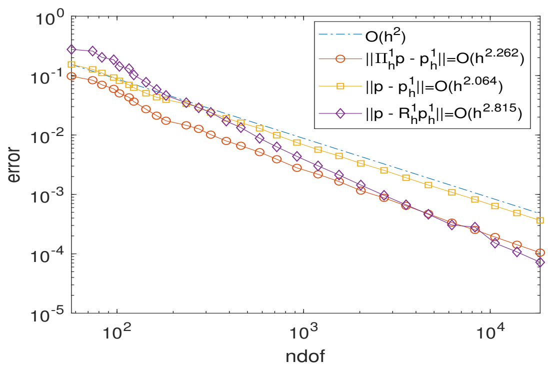

Fig. 6 Error curves for RT_1.

supercloseness and postprocessing operators are local, our superconvergence results can be adapted to Neumann and mixed boundary conditions. In practice, R_h^r can be extended to 3-dimensional RT elements in a straightforward way although the theoretical analysis in this paper may need significant modifications; see also [13] for numerical experiments on a different postprocessing operator for the lowest order RT elements in $\mathbb{R}^3$.

References

1. Arnold, D.N., Falk, R.S., Winther, R.: Finite element exterior calculus, homological techniques, and applications. Acta Numer. **15**, 1–155 (2006)
2. Arnold, D.N., Falk, R.S., Winther, R.: Finite element exterior calculus: from Hodge theory to numerical stability. Bull. Amer. Math. Soc. **47**(2), 281–354 (2010)
3. Bank, R.E., Xu, J.: Asymptotically exact a posteriori error estimators. I. grids with superconvergence. SIAM J. Numer. Anal. **41**(6), 2294–2312 (2003)
4. Bank, R.E., Xu, J.: Asymptotically exact a posteriori error estimators. II. general unstructured grids. SIAM J. Numer. Anal. **41**(6), 2313–2332 (2003)
5. Bank, R.E., Xu, J., Zheng, B.: Superconvergent derivative recovery for lagrange triangular elements of degree p on unstructured grids. SIAM J. Numer. Anal. **45**(5), 2032–2046 (2007)
6. Brandts, J.H.: Superconvergence and a posteriori error estimation for triangular mixed finite elements. Numer. Math. **68**(3), 311–324 (1994)
7. Brandts, J.H.: Superconvergence for triangular order k=1 raviart-thomas mixed finite elements and for triangular standard quadratic finite element methods. Appl. Numer. Math. **34**(1), 39–58 (2000)
8. Chen, L.: iFEM: an innovative finite element method package in Matlab (2009). University of California Irvine, Technical report
9. Chen, L., Holst, M., Xu, J.: Convergence and optimality of adaptive mixed finite element methods. Math. Comp. **78**(265), 35–53 (2009)
10. Dörfler, W.: A convergent adaptive algorithm for poisson's equation. SIAM J. Numer. Anal. **33**(3), 1106–1124 (1996)
11. Douglas J., J., Milner, F.A.: Interior and superconvergence estimates for mixed methods for second order elliptic problems. RAIRO Modél. Math. Anal. Numér. **19**(3), 397–428 (1985)
12. Douglas Jim, J., Roberts, J.E.: Global estimates for mixed methods for second order elliptic equations. Math. Comp. **44**(169), 39–52 (1985)
13. Dupont, T.F., Keenan, P.T.: Superconvergence and postprocessing of fluxes from lowest-order mixed methods on triangles and tetrahedra. SIAM J. Sci. Comput. **19**(4), 1322–1332 (1998)
14. Durán, R.: Superconvergence for rectangular mixed finite elements. Numer. Math. **58**(3), 287–298 (1990)
15. Huang, Y., Xu, J.: Superconvergence of quadratic finite elements on mildly structured grids. Math. Comp. **77**(263), 1253–1268 (2008)
16. Lakhany, A.M., Marek, I., Whiteman, J.R.: Superconvergence results on mildly structured triangulations. Comput. Methods Appl. Mech. Engrg. **189**, 1–75 (2000)
17. Li, B., Zhang, Z.: Analysis of a class of superconvergence patch recovery techniques for linear and bilinear finite elements. Numer. Methods Partial Differential Equations **15**(2), 151–167 (1999)
18. Li, Y.: Some convergence and optimality results of adaptive mixed methods in finite element exterior calculus (2019). Available as arXiv:1811.11143 [math.NA], to appear in SIAM J. Numer. Anal.
19. Li, Y.W.: Global superconvergence of the lowest-order mixed finite element on mildly structured meshes. SIAM J. Numer. Anal. **56**(2), 792–815 (2018)
20. Mitchell, W.F.: A comparison of adaptive refinement techniques for elliptic problems. ACM Trans. Math. Software **15**(4), 326–347 (1989)
21. Morin, P., Nochetto, R.H., Siebert, K.G.: Data oscillation and convergence of adaptive FEM. SIAM J. Numer. Anal. **38**(2), 466–488 (2000)
22. Naga, A., Zhang, Z.: A posteriori error estimates based on the polynomial preserving recovery. SIAM J. Numer. Anal. **42**(4), 1780–1800 (2004)
23. Raviart, P.A., Thomas, J.M.: A mixed finite element method for 2nd order elliptic problems, *Lecture Notes in Mathematics*, vol. 606, pp. 292–315. Springer, Berlin (1977)
24. Schatz, A.H., Sloan, I.H., Wahlbin, L.B.: Superconvergence in finite element methods and meshes that are locally symmetric with respect to a point. SIAM J. Numer. Anal. **33**(2), 505–521 (1996)

25. Shafarevich, I.R.: Basic algebraic geometry. 1. Varieties in projective space, thrid edition edn. Springer, Heidelberg (2013)
26. Wu, H., Zhang, Z.: Can we have superconvergent gradient recovery under adaptive meshes? SIAM J. Numer. Anal. **45**(4), 1701–1722 (2007)
27. Xu, J., Zhang, Z.: Analysis of recovery type a posteriori error estimators for mildly structured grids. Math. Comp. **73**(247), 1139–1152 (2004)
28. Zhang, Z., Naga, A.: A new finite element gradient recovery method: superconvergence property. SIAM J. Sci. Comput. **26**(4), 1192–1213 (2005)
29. Zienkiewicz, O.C., Zhu, J.: The superconvergent patch recovery and a posteriori error estimates. II. error estimates and adaptivity. Internat. J. Numer. Methods Engrg. **33**(7), 1365–1382 (1992)
30. Zienkiewicz, O.C., Zhu, J.Z.: The superconvergent patch recovery and a posteriori error estimates. I. the recovery technique. Internat. J. Numer. Methods Engrg. **33**(7), 1331–1364 (1992)